2009

THE WETTABILITY OF A DNAPL/SURFACTANT SOLUTION ON QUARTZ AND IRON OXIDE SURFACES

Ian L. Molnar
Western University

THE WETTABILITY OF A DNAPL/SURFACTANT SOLUTION ON QUARTZ AND IRON OXIDE SURFACES

(Spine title: THE WETTABILITY OF A DNAPL ON MINERAL SURFACES)
(Thesis format: Integrated-Article)

by

Ian L. Molnar

Graduate Program in Engineering Science

Department of Civil and Environmental Engineering

A thesis submitted in partial fulfillment
of the requirements for the degree of
Master of Engineering Science

School of Graduate and Postdoctoral Studies
The University of Western Ontario
London, Ontario, Canada

Abstract

THE WETTABILITY OF A DNAPL/SURFACTANT SOLUTION ON QUARTZ AND IRON OXIDE SURFACES

By

Ian L. Molnar

DNAPLs in the subsurface may contain surface-active compounds that impact DNAPL migration and distribution. A number of studies to-date have focused on the role surface active compounds play in altering the wettability of quartz sands without examining the implications for other minerals commonly present in the subsurface. This study aims to extend the understanding of DNAPL/surfactant wettability to iron oxide surfaces. Specifically the objective was to compare the changes in the wettability of quartz and iron oxide sands in a tetrachloroethylene/water system containing a representative organic base. Wettability was assessed through: contact angles; P_c-S curves; and a two-dimensional flow cell experiment. It was discovered that quartz and iron oxide surfaces may exhibit different wetting characteristics under similar subsurface conditions. At neutral pH the quartz was strongly NAPL-wetting while the iron oxide remained hydrophilic. This study concludes that the isoelectric point, the pH at which there is a net zero surface charge, plays a major role in governing cationic surfactant sorption.

Keywords: DNAPLs, PCE, wettability, subsurface, site remediation

Co-Authorship

The thesis was written in accordance with the guidelines and regulations for a manuscript format stipulated by the Faculty of Graduate Studies at the University of Western Ontario. The candidate conducted all the laboratory experiments; collected, interpreted and analyzed the experimental data under the close guidance and supervision of Dr. O'Carroll and Dr. Gerhard. The candidate wrote the manuscript draft of the follow chapters:

Chapter 3: The Wettability of a PCE/Organic Base Mixture on Quartz and Iron Oxide Surfaces
By Ian L Molnar, Denis M. O'Carroll and Jason I. Gerhard

Contributions:

Ian L Molnar:	performing the experiments, collected and interpreted experimental results, and wrote the draft of the paper.
Denis M. O'Carroll:	initiated the research topic, developed methodology, supervised the laboratory tests, assisted in data interpretation, and reviewed/revised the draft chapter
Jason I. Gerhard:	initiated the research topic, developed methodology, supervised the laboratory tests, assisted in data interpretation, and reviewed/revised the draft chapter

Acknowledgements

I must thank my two advisors, Denis O'Carroll and Jason Gerhard, for their patience, kindness and mentorship. It has been an incredible opportunity working with, and learning from the two of you over the past couple years and I can't thank you enough for all of this.

Thank you to everyone in the RESTORE research group for providing a safe and welcoming atmosphere (and free ice-cream), you have made research here a truly enjoyable experience. Thanks to Geremy Camps-Roach, Hardiljeet Boparai, Eun Jung Kim, Gaurav Goel and Stephanie Drake for their help and advice. I'd especially like to thank Chris Kocur, Stephanie MacPhee and Erin Cullen for their friendship.

I would not have made it without my family and friends that have provided love and support especially Nathan Newport and Laura Runciman. Thank you for being understanding and patient, it has meant a great deal to me. I am incredible lucky to have the family that I do: Paula, Lindsey and Marina Morritt and Sarah and Adam Charron.

Finally, my mother and father, Lou Anne and Robert Molnar are inspirations to me and the best parents I could ever ask for.

Funding for this project was provided by the Natural Sciences and Engineering Research Council of Canada as well as the Canadian Foundation for Innovation

Table of Contents

List of Tables

List of Figures

List of Appendices

List of Abbreviations, Symbols, Nomenclature

θ_A :	Denotes the contact angle measured as PCE moves across the solid surface
θ_r:	Denotes the contact angle measured as PCE recedes across the solid surface
γ :	Interfacial tension between two fluids (measured in mN/m)
DDA:	Dodecylamine
DNAPL:	Dense Non-Aqueous Phase Liquid
IFT:	Interfacial Tension
NAPL:	Non-Aqueous Phase Liquid
P_c:	Capillary Pressure
P_c-S:	Capillary Pressure-Saturation curve
PCE:	Tetrachloroethylene, also known as Perchloroethylene (C_2Cl_4)
r:	Radius of a pore throat

Chapter 1
Introduction

1.1. Problem Overview and Introduction

Groundwater comprises approximately 97% of the World's total supply of easily accessible freshwater [*World Health Organization*, 2006]. Groundwater's unique characteristic of being, on average, cleaner than surface water and its ubiquitous nature make it an appealing option for countries looking to expand their drinking water supplies. In fact, many countries rely almost exclusively on groundwater for drinking water sources including Austria and Denmark. These two countries receive 99% and 98% of their drinking water from groundwater sources respectively [*World Health Organization*, 2006].

When considering the heavy, and increasing, reliance on groundwater the importance of protecting these supplies becomes apparent. In particular, anthropogenic activities can put aquifers and the population reliant upon them at risk. These activities may include manufacturing, dry cleaning, degreasing and petro-chemical industries [*Environment Canada*, 1996]. The aforementioned activities use a class of chemicals knows as Non-Aqueous Phase Liquids (NAPLs) that are immiscible in water and, historically, were often disposed of improperly into the subsurface. Tetrachloroethylene (PCE), a denser-than-water NAPL (DNAPL) is a chlorinated solvent used by these industries that poses a particular problem due its widespread use, toxicity and persistence in the environment [*Environment Canada*, 1996].

In 1994, while no PCE was manufactured domestically in Canada, it is estimated that approximately 11,600 tonnes of PCE were imported, and 48% of that amount was used in the 3300 dry cleaners across the country that used PCE as a solvent [*Environment Canada*, 1996]. Once used, the PCE was then either volatilized to the air, disposed of as waste water or landfilled as a solid waste [*Environment Canada*, 1996]. Canada is home to an estimated 30,000 brownfield sites, and an unknown number of contaminated industrial sites still in operation, many of which exhibit pollution of soil and groundwater by hazardous industrial chemicals [*NRTEE*, 2003]. Based on a per capita scaling to US estimates, the life cycle costs for cleaning up only historical DNAPL sites in Canada are between $12B and $90B [*NRC*, 1999].

When released to the subsurface environment PCE acts as a persistent contaminant. Since PCE is a DNAPL it will enter the subsurface and, provided sufficient volume of DNAPL was spilled, migrate below the water table. The DNAPL source zone distribution is often extremely complex. It can pool on fine soil lenses, migrate into bedrock fractures or form disconnected ganglia blobs [*Mayer and Hassanizadeh*, 2005]. Then the PCE will slowly dissolve into the surrounding groundwater and may reach concentrations higher than is considered safe for human consumption. For example Health Canada sets a Maximum Acceptable Concentration for PCE at 0.03mg/L [*Health Canada*, 2008] however PCE is soluble in water up to 150mg/L [*Davis et al.*, 1997]. It is possible that 1L of PCE may contaminate up to 55 million liters of water above the Maximum Acceptable Concentration. As a result identifying and remediating sites contaminated with PCE is vital to protecting groundwater drinking supplies. However DNAPL remediation is

limited by lengthy processes and high costs due to complicated source zones and uncertain technologies [*Kavanaugh et al.*, 2003].

DNAPL sources zones are further complicated by unknown conditions both in the subsurface and the contaminant itself. Spatial changes in permeability, physical and geochemical heterogeneity as well as any surface active constituents within the NAPL all have a drastic effect on DNAPL distribution within the subsurface. However these factors are often unknown and the fundamental interactions between characteristics such as DNAPL constituents and source zone architecture are either poorly understood or ignored [*Mayer and Hassanizadeh*, 2005]. Physical heterogeneity in the subsurface has long been known to affect NAPL transport [*Brooks and Corey*, 1966; *Buckley and Leverett*, 1942]. Buckley and Leverett [1942] linked migration patterns of fluid flow through porous media with the size of pore throats and thus grain size distribution and packing arrangement. Brooks and Corey [1966] identified grain size distribution and entry pressure as two important parameters for characterizing the relationship between capillary pressure and saturation.

The effect of soil mineral composition on DNAPL flow remains poorly understood. While much effort has been made to understand the role of wettability in multi-phase flow, the link between subsurface wettability and geochemistry remains a poorly understood topic. Links have been made between surface roughness and wettability [*Morrow*, 1975] but the geochemical composition of those surfaces has been largely ignored until recently. Generic surfaces such as quartz [*Lord et al.*, 2000] are often used and assumed to be representative of the subsurface or studies are done on specific soils

but fail to draw fundamental links between wettability and the chemistry of the soils [*Harrold et al.*, 2001]. Ryder and Demond [2008] demonstrated the effect of geochemical heterogeneity on DNAPL transport properties and linked their findings with fundamental soil characteristics such as the oxygen content mineral surfaces.

Adding dimensions of complexity are any surface active constituents added to DNAPLs such as PCE to increase its working effectiveness. For example, surface active detergents are commonly added to solvents to increase their cleaning efficiencies [*Lange*, 1967]. By their very definition, surface active chemicals aggregate at any liquid/liquid interface and change the interfacial properties of the two liquids, which can then change their migration behavior in porous media. A number of studies have examined NAPL/surfactant mixtures and the fundamental interactions between surface active compounds and quartz sands [*Demond et al.*, 1994; *Desai et al.*, 1992; *Hsu and Demond*, 2007; *Lord et al.*, 2000; *Zheng and Powers*, 1999]. They linked the interactions to changes in DNAPL transport through quartz sand but did not address the geochemical heterogeneity found in the subsurface. The studies identified sorption of cationic surface active compounds to the negatively charged quartz surfaces as the primary mechanism for wettability alterations. While mineral soils tend to be predominantly quartz, other oxide surfaces are common and exhibit different surface charges than quartz, which may affect DNAPL transport in a different manner. Table 1 lists some minerals commonly found in the subsurface and what environments they are typically found in. While quartz is very common, Table 1 highlights the need to explore the effect of varying mineral composition, especially when considering the wettability of multi-component DNAPLs.

Table 1. Common Soil Minerals[1]

Name	Ubiquity in Soils	Environment
Quartz	Ubiquitous	Nearly all soils and parent materials
Hematite and Goethite	Ubiquitous	Well-drained, near surface soil
Feldspars	Rare to common	Wide variety of igneous and metamorphic rocks
Gibbsite	Common	Old, stable soils or feldspar pseudomorphs
Kaolinite	Ubiquitous	Desilication of 2:1 lays/feldspathic
Calcite	Common	Arid soils
Hydroxy-interlayered vermiculite	Ubiquitous	Acid, highly weathered soil surface horizons
Muscovite	Common	Granitic and high-grade metamorphic rocks

[1][*Feldman et al.*, 2008]

1.2. Study Objectives

The overall goal of this study is to improve understanding of DNAPL transport in representative, heterogeneous subsurface environments. Specifically, the relationships between mineral isoelectric points, DNAPL composition and wettability are explored. The first objective was to examine the advancing and receding contact angle of PCE on quartz and iron oxide plates in the presence of an organic base. Contact angles are measured over a range of pH values to delineate the effect of a surface's net charge on wettability and contact angle hysteresis in a PCE/water system. The quartz and iron oxide plates are employed as analogs of naturally occurring mineral surfaces found in the subsurface.

The second objective was to relate the contact angle results to the average behaviour of these fluid-fluid-solid systems over thousands of pores. Multi-step outflow experiments were used to measure the relationship between capillary pressure and water saturation on a representative elementary volume (REV) for these systems. In order to explore the impact of variable surface charges on quartz and iron oxide sands, the capillary pressure-saturation experiments were completed at contrasting pH values.

The third objective was to visually examine the differences in PCE migration between quartz and iron oxide sands in a small sandbox. The sandbox experiments were run under similar conditions to the contact angle and capillary pressure-saturation experiments. A light transmission visualization system was used to observe the presence and absence of PCE in both quartz and iron oxide sand regions. The sandboxes were packed in a way so as to allow side-by-side comparisons of the two sands when subjected to equal capillary pressure boundary conditions.

This systematic approach permits comparisons of behaviour of surfactant-modified PCE/water systems in two contrasting but common porous media systems, and the correlation of that behaviour from the pore scale to the REV scale to the small heterogeneity scale. In this manner, it is expected that conclusions can be drawn with regards to the influence of mineral surface types on the behavior of DNAPL in the presence of surface active compounds.

Chapter 2
Literature Review

2.1.Geochemical Heterogeneity in the Subsurface

The importance of electrostatic interactions between soil surfaces and surface active chemicals in NAPL waste mixtures has been well established in previous studies [*Chiappa et al.*, 1999; *Hsu and Demond*, 2007; *Lord et al.*, 2000; *Lord et al.*, 2005; *Zheng and Powers*, 1999; *Zheng et al.*, 2001]. Despite this, little work has been undertaken to account for the natural variability of soil minerals in the transport of NAPL waste mixtures, specifically the interactions between surface active chemicals and non-quartz soils. Table 1 illustrates the relative abundance of the major soil minerals and Table 2 provides a representative sample of work concerning surfactant-modified-NAPL transport in the subsurface. Charge development on a soil surface may cause cationic organic bases in solution to sorb to the surface. This buildup of surface active chemicals on the mineral may potentially alter the wettability of the system [*Zheng and Powers*, 1999]. Thus in order to predict alterations in NAPL wettability due to surface active molecules it is important to understand the electrostatic conditions that can occur on the surface of a mineral.

Electrical charge may develop on soil surfaces in two ways: permanent charges on the soil are developed primarily through isomorphic substitutions of ions of differing valencies within the soil matrix [*Sposito*, 1989], and variable (amphoteric) charges can develop through surface functional groups reacting with ions in solution [*Sposito*, 1989]. This study will largely ignore permanent charge development and focus predominantly

on the amphoteric surface charge as that is the predominant mechanism for charge development on minerals such as silica and iron oxides [*Singh and Uehara*, 1999].

Table 2: Selected NAPL Wettability Studies

Study	Solvent	Surfactant	Solid Substrate
[*Lord et al.*, 1997a; *Lord et al.*, 2000; *Lord et al.*, 1997b; *Lord et al.*, 2000; *Lord et al.*, 2005]	PCE/O-xylene	DDA,OA	Quartz
[*Hsu and Demond*, 2007]	PCE	DDA/OA mixture	Quartz
[*Powers et al.*, 1996]	Petroleum Products Creosote/Coal tar Neat solvents	Field NAPL Field NAPL None	Quartz Quartz Quartz
[*Demond et al.*, 1994]	O-xylene	CTAB	Quartz
[*Harrold et al.*, 2005]	TCE	DDA, octadeylamine, CTAB, OTMAB	Sandstone cores, Quartz plates
[*Harrold et al.*, 2001]	TCE	Unknown industrial mixture	Sandstone cores, Quartz plates
[*Powers and Tamblin*, 1995]	Isooctane	DDA, O-Toluidine, 2-Butoxyethanol, PBA	Quartz
[*Zheng and Powers*, 1999]	Creosote Coal Tars Petroleum Products	Field NAPLs	Quartz

The total electrical charge on a soil surface may be written as [*Sposito*, 1989]:

$$\sigma_{tot} = \sigma_o + \sigma_H + \sigma_{OS} + \sigma_{IS} \qquad [2\text{-}1]$$

All units of surface charge in [2-1] are expressed as moles of charge per kilogram (mol_c/kg). The total charge on the soil is given as σ_{tot}, σ_o is the permanent charge on the

soil surface (0 mol_c/kg in the case of a purely amphoteric mineral), σ_H is the net proton charge given as the difference in moles of hydrogen and hydroxide ions complexed at the surface, and σ_{OS} and σ_{IS} represent the charges from (not H^+ or OH^-) ions in solution that have complexed with the soil surface. This charge development is inversely correlated with pH. At low pH values the net charge will be positive and as the pH rises the charge becomes increasingly negative [*Singh and Uehara*, 1999]. The pH value where the net charge switches from positive to negative is different for every mineral oxide [*Sposito*, 1989]. For quartz sands, this value is approximately pH 2; below pH 2 the quartz carries a net positive charge and above it is increasingly negative [*Sposito*, 1989]. Iron oxide minerals generally switch from a net positive charge to a net negative charge at pH values of 6-8.5 [*Cornell*, 2003; *Parks*, 1965].

There are several ways to define the point at which a solid surface passes from a net positive to a net negative charge. The point of zero charge (PZC), or isoelectric point (IEPS), is commonly used to refer to the pH value where equation [2-1] equals 0 [*Cornell*, 2003; *Parks*, 1965; *Singh and Uehara*, 1999; *Sposito*, 1989]. The point of zero net proton charge (PZNPC) is the value at which the charges - due to complexed hydrogen and hydroxyl ions - are equal and is given as [*Sposito*, 1989]:

$$\sigma_H = q_H - q_{OH} = 0 \qquad [2\text{-}2]$$

In addition, the point of zero net charge (PZNC) is the point at which the number of sorbed cations and anions (not H^+ or OH^-) on the surface are equal [*Sposito*, 1989]. In a system with no surface complexation except for H^+ and OH^- ions, the three definitions are equivalent. For the purposes of this study, the term isoelectric point (IEPS) is used to

designate the pH value at which the surface switches from a net positive to a net negative charge.

Even a single type of mineral will have variations within the measured isoelectric point. Iron oxide minerals have a wide range of IEPS. Of the iron oxide minerals, goethite is the most common due to its high thermodynamic stability and can be found distributed from cool to humid climates [*Cornell,* 2003]. Goethite's isoelectric point can range from as low as 6 [*Parks*, 1965] up to 9.4 [*Cornell,* 2003]. In humid climates, goethite is commonly accompanied by hematite, the second most common iron oxide mineral and has a similar isoelectric point [*Cornell,* 2003; *Parks*, 1965]. Other important mineral oxides in the ground, such as gibbsite, can have an isoelectric point in the range of 4-5 [*Parks*, 1965].

2.2.Introduction to DNAPL Contamination and Transport

Sites contaminated with dense non-aqueous phase liquids (DNAPLs) pose a particular risk to groundwater sources due to their toxicity and resistance to remediation efforts. Compounding the problem is the large number of DNAPL contaminated sites that are currently known to exist. It is estimated that the number of DNAPL contaminated sites in the U.S.A. alone is between 15,000 and 25,000 [*Kavanaugh*, 2003]. These sites may include chemicals such as petroleum waste products, coal tar, creosote and chlorinated solvents. Despite the prevalence and risk these sites create for the surrounding environment there have been no reported cases of large DNAPL sites where remediation has been restored to drinking water standards [*National Research Council*, 2005]. Indeed,

the presence of free phase DNAPL on a site may pose a worst-case remediation scenario [*Macdonald and Kavanaugh*, 1994].

Part of the difficulty encountered with DNAPLs is that, as an immiscible liquid with relatively low water solubility, free-phase NAPL may serve as a long-term source of groundwater contamination, slowly dissolving into the surrounding environment over decades or longer. Understanding the DNAPL source zone, the soil matrix and the DNAPL source architecture, is important for effective remediation efforts yet remains poorly understood [*Kavanaugh,* 2003]. In the following section, an overview of the transport mechanisms of immiscible liquids in the subsurface will be presented.

Soils may have a wide distribution of grain and pore sizes arrayed in a complex manner. Preferential pathways and large scale heterogeneities are difficult to detect and impact subsurface DNAPL transport. In an effort to represent DNAPL transport through this complex medium mathematically, the subsurface is often idealized as a bundle of tubes [*Mayer and Hassanizadeh*, 2005]. Each tube represents a pore throat between sand grains. As a liquid moves between soil grains and through the pore throats it can be considered to be moving through a tube of a radius r. Figure 1 shows a front of NAPL moving through a tube displacing the aqueous (wetting) phase.

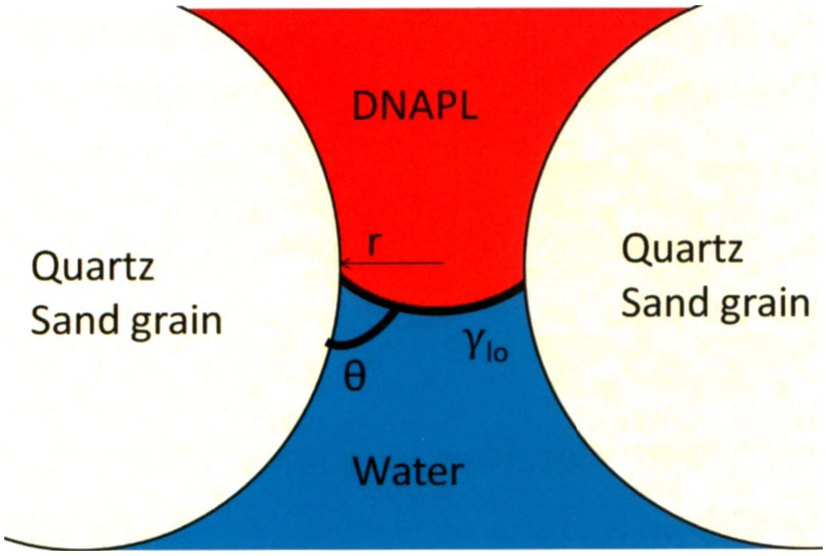

Figure 1: A non-wetting phase liquid displacing the wetting phase liquid.

The pressure difference between the DNAPL and water, known as the capillary pressure, can be given by the Laplace-Young equation [*Bear*, 1979]:

$$P_c = \gamma \left[\frac{1}{R_1} + \frac{1}{R_2}\right] \qquad [2\text{-}3a]$$

The interfacial tension of the fluid/fluid interface is γ and R_1 and R_2 are the principle radii of curvature. The equation [2-3a] may be rewritten where the radius of the interface is described as the cosine of the contact angle. This new equation is shown in [2-3b] and is the capillary pressure required for the DNAPL to displace water from the pore throat. This capillary pressure in [2-3b] is related to: the interfacial tension between the water and DNAPL; the contact angle formed at the DNAPL/water/solid interface; and the size of the pore throat.

$$P_c = \frac{2\gamma_{lo}\cos\theta}{r} \qquad [2\text{-}3b]$$

Where γ_{lo} is the interfacial tension between the two fluids, cos(θ) is the contact angle of the fluid/fluid/solid interface and r is the radius of the pore throat. P_c, the capillary pressure, is defined as the difference in pressure between two immiscible fluid phases separated by a curved interface [*Mercer and Cohen*, 1990]:

$$P_c = P_N - P_W \qquad [2\text{-}4]$$

Where P_N is the pressure in the organic phase, typically identified as the non-wetting phase, and P_W is the pressure in the aqueous phase, typically identified as the wetting phase.

While the relationships [2-3a] and [2-3b] are idealizations of porous media systems, neither equation accounts for the natural variability in pore sizes and shapes, it illustrates the dependence of displacement pressure on IFT, θ and r. When considering DNAPL entry into a volume of porous material a different relationship is required to predict the capillary pressure. It is necessary to account for the wide range of pore sizes, grain shapes and contact angles. Thus well graded sand may possess a wide range of displacement pressures and a different relationship is needed to express this [*Mayer and Hassanizadeh*, 2005]. A number of constitutive relationships have been developed between the capillary pressure applied and the saturation of water in a representative soil sample [*Brooks and Corey*, 1966; *van Genuchten*, 1980]. As the capillary pressure between an aqueous and NAPL phase increases very little, if any, water will be initially displaced until the displacement pressure is reached. Once passing the displacement pressure water begins to drain from a sand sample until the saturation approaches residual. At residual saturation water will cease draining out of a sample despite increases in capillary pressure. Figure 2

illustrates this relationship by showing the typical shape of a capillary pressure-saturation (P_c-S) curve.

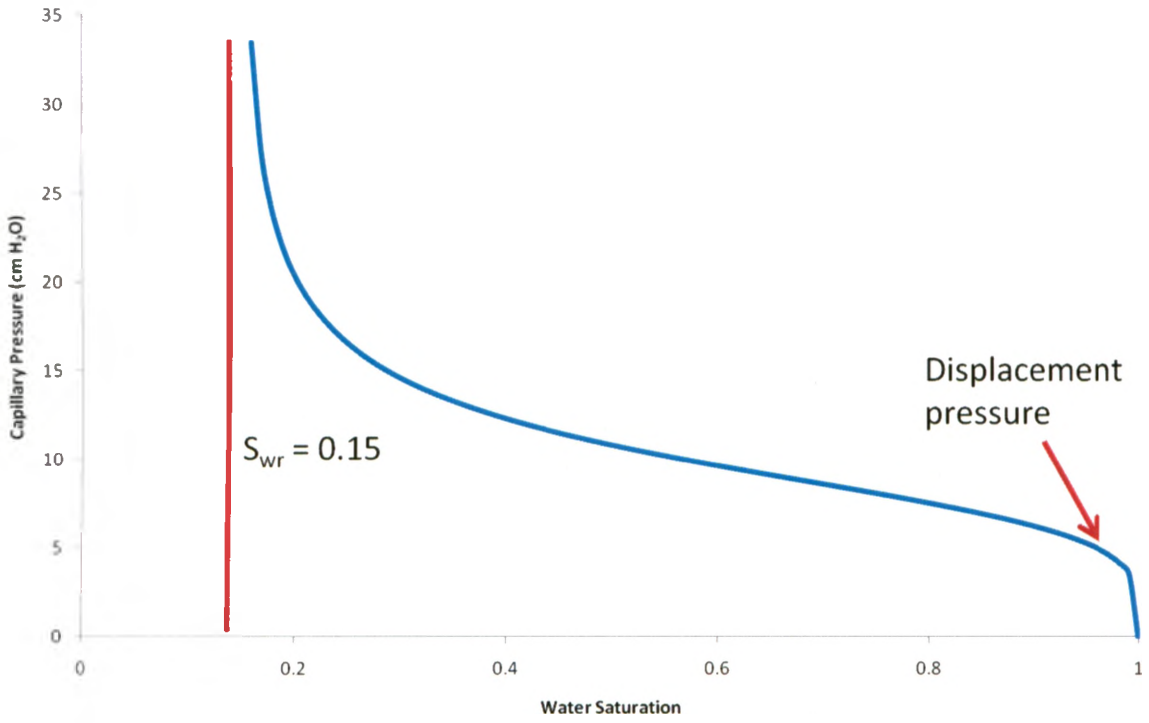

Figure 2: The shape of a typical P_c-S curve.

The aforementioned relationships are crucial when predicting patterns of DNAPL migration [*Gerhard and Kueper*, 2003] and for understanding source zone architecture [*O'Carroll et al.*, 2004]. Two common functions are employed to describe P_c-S [*Brooks and Corey*, 1966; *van Genuchten*, 1980]. In this study the van-Genuchten relationship is used to construct and compare P_c-S for systems of interest.

With the wide range of DNAPLs, interfacial tensions and contact angles in the subsurface, it can be useful to directly compare capillary pressure-saturation curves through a method known as Leverett scaling [1941]. The relationship developed by

Leverett [1941] to scale the displacement pressures to changes in interfacial tension or soil properties is given as:

$$\left[\frac{P_c(S_e)}{\gamma_{lo}}\sqrt{\frac{k}{n}}\right]_1 = \left[\frac{P_c(S_e)}{\gamma_{lo}}\sqrt{\frac{k}{n}}\right]_2 \quad [2\text{-}5]$$

In [2-5] k is the intrinsic permeability, n represents porosity of the soil and S_e is the effective saturation:

$$S_e = \frac{S_w - S_{wr}}{1 - S_{wr}} \quad [2\text{-}6]$$

Where S_w is the saturation of water in the soil sample and S_{wr} is the residual saturation of water. The residual saturation is the point at which no additional water can be drained from a sample of sand despite increases in capillary pressure. Figure 2 illustrates the irreducible water saturation and is shown to be at 15% saturation for the particular drainage curve. Converting from real saturation to effective saturation is a useful measure to calculate as it allows direct comparison of P_c-S relationships between systems with different residual saturations. For two soils containing similar permeabilities and porosities [2-5] may be simplified by eliminating k and n from the equation and scaling the drainage curve based on interfacial tension alone.

Modifications have been made to [2-5] to account for changes in contact angle as well as interfacial tension [*Demond et al.*, 1994; *Desai et al.*, 1992]:

$$P_c(S_e)_2 = P_c(S_e)_1 \frac{(\gamma_2 \cos\theta_r Z(\theta))_2}{(\gamma_1 \cos\theta_r Z(\theta))_1} \quad [2\text{-}7]$$

Where the $Z(\theta)$ and θ_r terms were introduced by Melrose [1965] and Morrow[1975] respectively to better account for actual pore geometry. The term $Z(\theta)$ was introduced by Melrose [1965] to account for differences in interface curves between the capillary tube model and a real system. Contact angle θ_r is the contact angle corrected for roughness [*Morrow*, 1975]. This correction for roughness on the contact angle is necessary because the intrinsic contact angle measured on a flat plate and the operational contact angle observed during DNAPL transport are often quite different. The contact angle roughness corrections developed by Morrow [1975] are shown in [2-8] and [2-9].

$$0^o < \theta_{int} < 21.6^o \quad \theta_r = 0 \qquad [2\text{-}8]$$

$$21.6^o < \theta_{int} < 87.6^o \quad \theta_r = 0.5\exp(0.05\theta_{int}) - 1.5 \qquad [2\text{-}9]$$

Desai et al. [1992] successfully used [2-7] to predict P_c-S curves in a hydrophilic air/water/quartz system containing the surface active chemical CTAB. The work of Demond et al. [1994] applied the equation [2-7] to predict the behavior of NAPL-wet o-xylene/water/quartz systems containing CTAB and found [2-7] provided a reasonable fit for displacement pressures yet failed to capture the shape of the curves. Both incorporated this roughness correction factor successfully to predict capillary pressure-saturation relationships in a system containing surface active chemicals.

It is also possible to scale P_c-S curves for fractionally wet systems where a mixture of hydrophilic and hydrophobic sand grains are simultaneously present [*O'Carroll et al.*, 2005]. The contact angle used when predicting fractionally wet P_c-S relationships is

known as the apparent contact angle. An apparent contact angle for a fractionally wet system may be derived by using the Cassie equation [1948]:

$$Cos(\theta) = f_1 \cos(\theta_1) + f_2 \cos(\theta_2) + \ldots f_i \cos(\theta_i) \qquad [2\text{-}10]$$

Where f_i represents the surface area fraction for a certain material and θ_i is the contact angle on that material.

Constitutive relationships can accurately describe NAPL behavior in a representative elementary volume (REV) of soil. While these relationships are unique for each system it has been shown that they can be accurately scaled to predict transport behavior in other systems with different interfacial properties [*Demond et al.*, 1994]. The next section will further consider the impact these interfacial properties have on DNAPL transport and the factors that can alter them.

2.3.Interfacial Properties of DNAPLs in the Subsurface

The two major interfacial properties that affect DNAPL transport are interfacial tension and contact angle. Interfacial tension between two fluids is due to an imbalance of forces at the fluid/fluid interface. At this interface there are two types of forces acting on each fluid phase; cohesive and adhesive forces. Cohesive forces are the attractive forces between molecules in a single liquid phase and adhesive forces are the forces holding two liquids together at an interface. A molecule residing at the interface between two fluid phases will be subject to a net force and will possess an excess of potential energy holding it at the interface [*Mayer and Hassanizadeh*, 2005]. This excess potential energy

is also known as interfacial tension. The relationship between adhesive and cohesive forces is [*Martin and Fulton*, 1958].

$$W_{ab} = \gamma_a + \gamma_b - \gamma_{ab} \qquad [2\text{-}11a]$$

Where W_{ab} represents the adhesive force between fluids a and b, γ_a and γ_b are the cohesive forces for each fluid and γ_{ab} is the interfacial tension (IFT). Rearranging [2-11a] to isolate IFT gives:

$$\gamma_{ab} = \gamma_a + \gamma_b - W_{ab} \qquad [2\text{-}11b]$$

Equation [2-11b] illustrates that IFT may be altered through two primary routes:

1) Additives may be in the DNAPL or water phase, which would increase the cohesive force, raising IFT. For example increasing the ionic strength of an aqueous solution increases the cohesive force within the liquid and would raise the IFT of the solution [*Barranco Jr et al.*, 1997]. Barranco Jr. et al. [1997] noted that in pure carbon tetrachloride and trichloroethylene solutions the interfacial tension increased by approximately 10 dynes/cm when the ionic strength of the solution increased from 2.0×10^{-6}M to 1M. Lord et al. [1997b] and Standal et al. [1999] both examined the effect of counterions on the IFT in systems containing surface active compounds. Lord et al. [1997b] noted a slight drop in IFT with increasing NaCl concentration that was completely independent of the presence of the surface active compound. This was most likely due to enhancing the surface activity of impurities within the o-xylene or water [*Lord et al.*, 1997b]. Standal et al. [1999] also noted a slight drop in IFT in isooctane/water/surfactant systems with increasing NaCl concentration. They noted,

however, that increasing the salt content of the aqueous phase 'salts out' organic compounds from the water causing the surface active compounds to partition back into the isooctane[*Standal et al.*, 1999]. It was also shown that the presence of divalent salts further increased the 'salting out' effect over monovalent salts [*Standal et al.*, 1999].

2) There may be additives in the DNAPL or water that would increase the adhesive force, thereby lowering IFT. A number of studies have shown the role industrial additives play in lowering the interfacial tension of NAPL/Water systems [*Dou et al.*, 2008; *Harrold et al.*, 2001; *Harrold et al.*, 2003; *Harrold et al.*, 2005; *Hsu and Demond*, 2007; *Lord et al.*, 2000; *Lord et al.*, 1997b; *Lord et al.*, 2005; *Nellis et al.*, 2009]. Dry cleaners may add in surfactants to increase the detergency of the solvent being used [*Lange*, 1967; *Martin and Fulton*, 1958] or solvents used for degreasing may dissolve surface active compounds encountered throughout their working life. These surfactants, by definition, build up at the interface between the oil phase and water phase and change the interfacial tension [*Martin and Fulton*, 1958]. Lord et al. [2000] showed that dodecylamine (DDA), a weak organic base, built up at the NAPL/water interface when the DDA was predominantly cationic. The acid/base reaction for DDA is given as:

$$RNH_3^+ = H^+ + RNH_2\,,\ K_a = 10^{-10.6} \qquad [2\text{-}12]$$

And the distribution of DDA between the between the organic and aqueous phases may be described as:

$$D = \frac{(RNH_2)_o}{(RNH_3^+)+(RNH_2)} \qquad [2\text{-}13]$$

At low pH values the DDA molecule would align itself so that the cationic functional group was present in the aqueous phase while the hydrocarbon tail remained in the NAPL. Thus as pH increased, the DDA deprotonated and moved away from the NAPL/water interface (Figure 3). This shift away from the interface was accompanied by a general migration of DDA from the aqueous to the NAPL phases. The interfacial tension is a strong function of system pH in the presence of weak organic acids and bases [*Barranco Jr and Dawson*, 1999; *Lord et al.*, 1997a; *Lord et al.*, 2000].

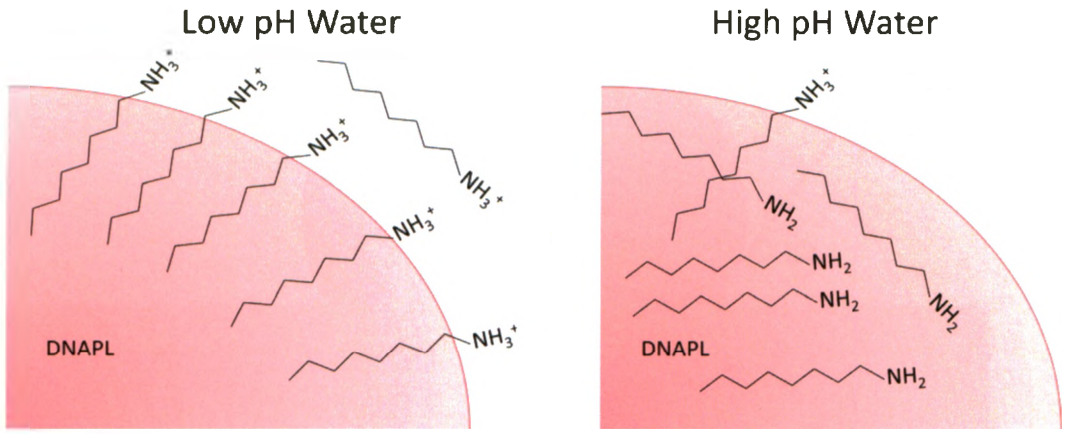

Figure 3: An illustration of DDA behaviour at a DNAPL/water interface at low and high pH values.

Numerous field samples have been found to have interfacial tensions that were lowered by surface active chemicals [*Birak and Miller*, 2009; *Dou et al.*, 2008; *Harrold et al.*, 2003; *Nellis et al.*, 2009] as well as altered wettability. Intermediate to NAPL-wetting behavior has been identified for several field samples [*Harrold et al.*, 2001; *Harrold et al.*, 2003; *Harrold et al.*, 2005; *Jackson and Dwarakanath*, 1999] and the process through which wettability may switch from hydrophilic to intermediate wetting or hydrophobic is discussed below.

Another major factor controlling DNAPL migration through the subsurface is the wettability of the aquifer material. Wettability is a term used to describe the preferential wetting of a solid surface by one fluid in the presence of another [*Martin and Fulton*, 1958]. The single most common measure of wettability is the contact angle [*Morrow*, 1990]. Consider a drop of DNAPL on a smooth plate surrounded by water (Figure 4) where γ_{os} is the surface tension between the DNAPL and the solid surface, γ_{ws} is the surface tension between the water and the solid surface and γ_{wo} is the interfacial tension between the water and organic phase as discussed in section 2.2.

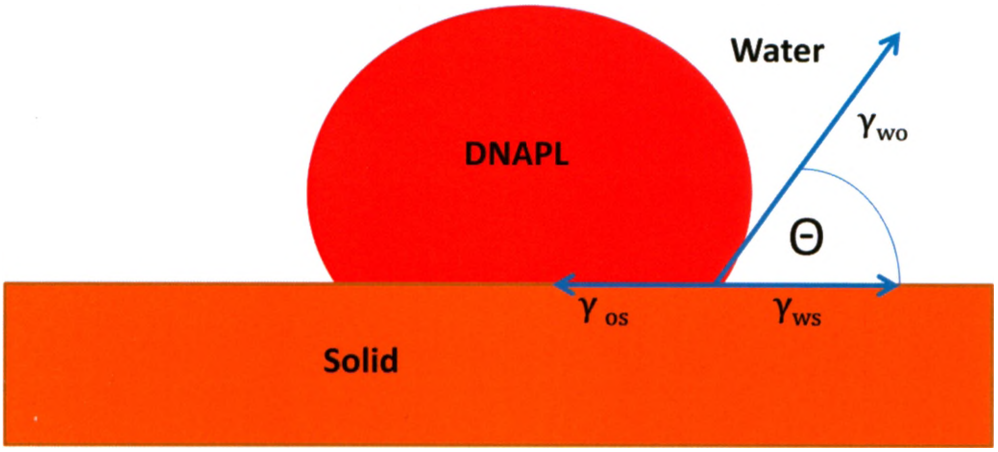

Figure 4: Contact angle of DNAPL on a solid surface.

A force balance between the three tensions can be written as [*Martin and Fulton*, 1958]:

$$\gamma_{os} = \gamma_{ws} + \gamma_{wo}\cos(\theta) \qquad [2\text{-}14]$$

Equation [2-14] can be used to describe how the DNAPL droplet will behave on a solid surface. As the contact angle passes from $\theta<90^{\circ}$ to $\theta>90^{\circ}$ the wettability switches from water wetting to intermediate to NAPL wetting. Contact angles (θ) below 70° are indicative of a water-wet, or hydrophilic, solid surface whereas $\theta>110^{\circ}$ suggest a NAPL

wetting surface. Contact angle θ values between 70° and 110° are intermediate wetting systems [*Morrow*, 1975]. At a θ of 90° the surface energies of the organic and aqueous phases are similar with respect to the solid surface so the solid surface does not distinguish between either fluid. Equation [2-14] describes the interactions between surface energies as the switch between wettabilities occur.

While the surface tensions of water/solid and NAPL/solid systems are difficult to measure, the contact angle is simple to measure and provides an unambiguous measure of the system's wettability [*Ryder*, 2007]. The contact angle is a function of the direction of saturation change [*Desai et al.*, 1992]. Water drainage and water imbibition in porous media is analogous to the DNAPL droplet advancing and receding over the solid surface in a contact angle measurement. The differences in advancing and receding contact angle are referred to as hysteresis and affect the water drainage/imbibition characteristics. In a hysteretic system the NAPL-advancing contact angle will always be smaller than the NAPL-receding contact angle with the stationary contact angles somewhere in between the two values [*Mercer and Cohen*, 1990].

The chemical constituents of the NAPLs may affect subsurface wettability in addition to IFT. Powers et al. [1996] examined a series of NAPLs including: gasoline, diesel fuel with a wide range of organic compounds, and 'neat' NAPLs, such as toluene and trichloroethylene (TCE). It was determined that NAPLs with high-molecular weight compounds, such as creosote, or surface active chemicals had a greater effect on the wettability of sands than the low-molecular weight compounds such as TCE and toluene [*Powers et al.*, 1996]. Morrow [1990] reviewed the literature surrounding the

composition of oils and compared that to soil wettability and oil recovery and concluded that the presence of asphaltenes, high weight molecular compounds, was found to be commonly associated with alterations in subsurface wettability at oil-field sites. The extent of alteration in subsurface wettability was linked with the efficiency of oil-recovery. This linkage showed highly oil-wetting soils to have low recovery efficiencies with maximum recovery efficiencies occurring at neutral wetting conditions. This was because the soil had no preference for either oil or water and the aqueous and organic phases were able to displace the opposing phase from the soil grains [*Morrow*, 1990]. A study by Zheng et al. [2001] further examined role asphaltenes played and found at low concentrations the wettability alterations were linked to electrostatic and van der waal interactions, and at higher concentrations asphaltene precipitate on the soil dominated behavior.

Wettability has been shown to be altered by chemical constituents typically associated with the organic phase [*Jackson and Dwarakanath*, 1999], the aqueous phase [*Barranco Jr and Dawson*, 1999; *Barranco Jr et al.*, 1997; *Chiappa et al.*, 1999] and properties of the solid phase [*Hassenkam et al.*, 2009; *Morrow*, 1975; *Ryder and Demond*, 2008]. Fundamental interactions between the three phases are shown to govern wettability in the aforementioned studies. Buckley and Liu [1998] proposed four fundamental interactions that govern wettability with DNAPLs: 1) polar interaction between high molecular weight additives such as asphaltene molecules and mineral surfaces in the absence of water, 2) precipitation of asphaltenes at the interface, 3) acid/base interactions that affect surface charge at oil/water and water/mineral surfaces, 4) ion-binding or specific interactions between charged sites and di- or trivalent cations.

The third mechanism described above is thought to be a significant factor determining the wettability of NAPL/water/solid systems [*Buckley et al.*, 1998]. As quartz sand has a net negative charge above a pH of 2, and a net positive charge below pH 2 [*Sposito*, 1989], cationic compounds will perferentially sorb to the quartz sand at typical subsurface pH values.

Several studies have linked contact angle changes to the sorption of cationic surface active chemicals to negatively charged sites on a quartz surface [*Demond et al.*, 1994; *Desai et al.*, 1992; *Harrold et al.*, 2005; *Hsu and Demond*, 2007; *Lord et al.*, 2000; *Lord et al.*, 2005; *Zheng and Powers*, 1999]. The general trend observed was that, at low pH values where the quartz was weakly negative, the system remained strongly hydrophilic due to limited sites for cationic surfactant sorption. As the pH was increased to near neutral values cationic surfactants would sorb to the solid surface switching the wettability to intermediate or NAPL wetting. As the pH increased further, the mechanism described in Figure 3 became dominant and the surface switched back to water wetting as the surfactant partitioned back in to the NAPL phase. Zheng et al. [1999] hypothesized that the presence of organic bases was necessary to alter the wettability of quartz surfaces. The study found a correlation between the amount of organic base in the NAPL and the wettability of the sand but found that more NAPLs wet the quartz surface at low pH values than at neutral. This seeming contradiction between Zheng et al. [1999] and can be explained by examining the strength of the organic bases in solution. Stronger organic bases will be protonated at higher pH values and will strongly sorb to the quartz surface across a range of pH's. However, even high concentrations of weak organic bases will fail to alter the wettability of quartz if the surface active chemicals lack a cationic

charge [*Zheng and Powers*, 1999]. Alternatively, sufficiently high concentrations of surface active chemicals may form a bilayer on the quartz surface causing the wettability to switch from NAPL-wetting to water-wetting. It is also possible for a single surface to exhibit non-homogeneous wetting either due to changes in the surface composition or non-uniform sorption of surface active chemicals [*Harrold et al.*, 2001].

While organic bases have been shown to consistently alter wettability, organic acids, which are predominantly anionic, have not[*Lord et al.*, 1997a]. Lord et al. [1997a] noted that in the pH range 3 – 9, quartz remained hydrophilic in the presence of octanoic acid due to anionic octanoic acid not sorbing to the quartz surface. It was hypothesized that divalent cations could provide a 'bridge' for anionic molecules to sorb to negatively charged surfaces such as quartz [*Chiappa et al.*, 1999]. Chiappa et al. [1999] noted that the presence of $CaCl_2$ in solution enhanced the adsorption of negatively charge polymer molecules to a negatively charge quartz surface. However, the presence of organic acids enhances the surface activity of organic bases in a NAPL/water/quartz solution [*Hsu and Demond*, 2007]. Mixtures of DDA/octanoic acid have been shown to have a much greater affect on wettability than would be expected as octanoic acid is not linked to changes in contact angles. As octanoic acid was added to a PCE/water/quartz system containing DDA the wettability switched from weakly water wet to NAPL wetting and this change was postulated to be due to the formation of DDA/OA complexes.

Given the prevalence of surface active compounds in organic liquid mixtures [*Jackson and Dwarakanath*, 1999] (e.g., asphaltenes, organic acids/bases and surfactants) the ability of acid/base interactions to alter subsurface wettability is a topic that requires

more attention. Most work completed to-date concerning the wettability of DNAPL waste mixtures focuses almost solely on understanding the wettability of quartz surfaces (Table 2) despite the prevalence of other minerals in the subsurface such as iron oxides. In addition, few studies have linked contact angle behaviour to capillary pressure-saturation curves [*Demond et al.*, 1994; *Desai et al.*, 1992; *Lord et al.*, 2000; *Lord et al.*, 2005; *O'Carroll et al.*, 2004] and fewer still have correlated the contact angles and capillary pressure-saturations curves to two dimensional DNAPL distribution [*O'Carroll et al.*, 2004] and none have done that using a DNAPL/surface active chemical mixture.

2.4.References

Health Canada (2008), Guidelines for Canadian Drinking Water Quality, edited.

Barranco Jr, F.T., and H. E. Dawson (1999), Influence of aqueous pH on the interfacial properties of coal tar, *Environmental Science and Technology*, *33*(10), 1598-1603.

Barranco Jr, F. T., et al. (1997), Influence of aqueous pH and ionic strength of the wettability of quartz in the presence of dense non-aqueous-phase liquids, *Environmental Science and Technology*, *31*(3), 676-681.

Bear, J. (1979), *Hydraulics of Groundwater*, McGraw-Hill, New York.

Birak, P. S., and C. T. Miller (2009), Dense non-aqueous phase liquids at former manufactured gas plants: Challenges to modeling and remediation, *Journal of Contaminant Hydrology*, *105*(3-4), 81-98.

Brooks, R. H., and A. T. Corey (1966), Properties of porous media affecting fluid flow, *American Society of Civil Engineers Proceedings, Journal of the Irrigation and Drainage Division*, *92*(IR2), 61-88.

Buckley, J., and Y. Liu (1998), Some mechanisms of crude oil/brine/solid interactions, *Journal of Petroleum Science and Engineering*, *20*(3-4), 191-202.

Buckley, J., and Lord, DL (2003), Wettability and morphology of mica surfaces after exposure to crude oil, *Journal of Petroleum Science and Technology*, *39*(3-4), 261-273.

Buckley, S. E., and M. C. Leverett (1942), Mechanism of fluid displacement in sands, *American Institute of Mining and Metallurgical Engineers -- Transactions -- Petroleum Development and Technology Division*, *146*, 107-116.

Cassie, A.B.D. (1948), Permeability to water and water vapour of textiles and other fibrous materials. *Discuss. Faraday Soc.* 3 (11), 239– 243.

Chiappa, L., et al. (1999), Polymer adsorption at the brine/rock interface: the role of electrostatic interactions and wettability, *Journal of Petroleum Science and Engineering*, *24*(2-4), 113-122.

Cornell, R. M., Schwetmann, U., (2003), *The iron oxides : structure, properties, reactions, occurrences and uses*, 2 ed., WILEY-VCH Verlag GmbH & Co. KGaA, Weinheim.

Davis, E. L., et al. (1997), Ground water issue [electronic resource]: how heat can enhance in-situ soil and aquifer remediation--important chemical properties and guidance on choosing the appropriate technique, E.P.A., Office of Solid Waste and Emergency Response, Washington, D.C.

Demond, A. H., et al. (1994), Effect of cationic surfactants on organic liquid-water capillary pressure-saturation relationships, *Water Resources Research*, *30*(2), 333-342.

Desai, F. N., et al. (1992), The influence of surfactant sorption on capillary pressure-saturation relationships, in *Transport and Remediation of Subsurface Contaminants: Colloidal, Interfacial and Surfactant Phenomena*, edited, pp. 133-148, American Chemical Society, Washington, D.C.

Dou, W., et al. (2008), Characterization of DNAPL from the US DOE Savannah River site, *Journal of Contaminant Hydrology*, *97*(1-2), 75-86.

Dwarakanath, V., et al. (2002), Influence of wettability on the recovery of NAPLs from alluvium, *Environ. Sci. Technol.*, *36*(2), 227-231.

Feldman S.B., C. S., and Lucian W. Zelazny (2008), Soil Mineralogy, in *Encylopedia of Soil Science*, edited by W. Chesworth, pp. 678-685, Springer, Dordrecht.

Government of Canada (1996), Tetrachloroethylene Regulations - A Strategic Options Report, Environment Canada.

Gerhard, J. I., and B. H. Kueper (2003), Capillary pressure characteristics necessary for simulating DNAPL infiltration, redistribution, and immobilization in saturated porous media, *Water Resources Research*, *39*(8), 17.

Harrold, G., et al. (2001), Wettability changes in trichloroethylene-contaminated sandstone, *Environmental Science and Technology*, *35*(7), 1504-1510.

Harrold, G., et al. (2003), Changes in interfacial tension of chlorinated solvents following flow through UK soils and shallow aquifer material, *Environ. Sci. Technol.*, *37*(9), 1919-1925.

Harrold, G., et al. (2005), The impact of additives found in industrial formulations of TCE on the wettability of sandstone, *Journal of Contaminant Hydrology*, *80*(1-2), 1-17.

Hassenkam, T., et al. (2009), Probing the intrinsically oil-wet surfaces of pores in North Sea Chalk at subpore resolution, *Proceedings of the National Academy of Sciences of the United States of America*, *106*(15), 6071-6076.

Hirasaki, G. J. (1991), Wettability: fundamentals and surface forces, *SPE Formation Evaluation*, *6*(2), 217-226.

Hsu, H.-L., and A. H. Demond (2007), Influence of organic acid and organic base interactions on interfacial properties in NAPL-water systems, *Environmental Science and Technology*, *41*(3), 897-908.

Jackson, R. E., and V. Dwarakanath (1999), Chlorinated degreasing solvents: Physical-chemical properties affecting aquifer contamination and remediation, *Ground Water Monit. Remediat.*, *19*(4), 102-110.

Kavanaugh, M.C. et al. (2003), The DNAPL remediation challenge: Is there a case for source depletion?, edited by Office of Research and Development, United States Environmental Protection Agency, Cincinnati

Lange, H. (1967), Physical chemistry of cleansing action, in *Solvent Properties of Surfactant Solutions*, edited by K. Shinoda, pp. 117-188, Marcel Dekker, Inc New York.

Leverett, M. C. (1941), Capillary behavior in porous solids, *American Institute of Mining and Metallurgical Engineers -- Petroleum Development and Technology*, *142*, 152-168.

Lord, D.L., et al. (1997a), Influence of organic acid solution chemistry on subsurface transport properties. 2. Capillary pressure−saturation, *Environmental Science and Technology*, *31*(7), 2052-2058.

Lord, D.L., et al. (1997b), Influence of organic acid solution chemistry on subsurface transport properties. 1. surface and interfacial tension, *Environmental Science and Technology*, 31(7), 2045-2051.

Lord, D.L , et al. (2000), Effects of organic base chemistry on interfacial tension, wettability and capillary pressure in multiphase subsurface waste systems, *Transport in Porous Media*, *38*(1-2), 79-92.

Lord, D. L., et al. (2005), Comparison of capillary pressure relationships of organic liquid-water systems containing an organic acid or base, *Journal of Contaminant Hydrology*, *77*(3), 195-208.

Macdonald, J. A., and M. C. Kavanaugh (1994), Restoring contaminated groundwater – an achievable goal, *Environ. Sci. Technol.*, *28*(8), A362-&.

Martin, A. R., and G. P. Fulton (1958), *Drycleaning Technology and Theory*, Textile Book Publishers, New York.

Mayer, A. S., and S. M. Hassanizadeh (2005), *Soil and Groundwater Contamination: Nonaqueous Phase Liquids*, American Geophysical Union, Washington, D.C.

Melrose, J. C. (1965), Wettability as related to capillary action in porous media, *Society of Petroleum Engineers -- Journal*, *5*(3), 259-271.

Mercer, J. W., and R. M. Cohen (1990), A review of immiscible fluids in the subsurface: properties, models, characterizations and remediation, *Journal of Contaminant Hydrology*, *6*(2), 107-163.

Morrow, N. R. (1975), The effects of surface roughness on contact angle with special reference to petroleum recovery, *Journal of Canadian Petroleum Technology*, *14*(4), 42-53.

Morrow, N. R. (1990), Wettability and Its effect on oil recovery, *Journal of Petroleum Technology*, *42*(12), 1476-1484.

National Research Council (1999), *Ground water and soil cleanup: improving management of persistent contaminants*, 1 ed., The National Academies Press, Washington, D.C.

National Research Council (2005), *Contaminants in the Subsurface: Source Zone Assessment and Remediation*, 1 ed., The National Academies Press, Washington D.C.

Nellis, S. R., et al. (2009), Surface and interfacial properties of nonaqueous-phase liquid mixtures released to the subsurface at the hanford site, *Vadose Zone J.*, *8*(2), 343-351.

NRTEE (2003), Cleaning up the past, building the future: a national brownfield redevelopment strategy for Canada, 9 pp, Government of Canada.

O'Carroll, D. M., et al. (2004), Infiltration of PCE in a system containing spatial wettability variations, *Journal of Contaminant Hydrology*, *73*(1-4), 39-63.

O'Carroll, D. M., et al. (2005), Prediction of two-phase capillary pressure-saturation relationships in fractional wettability systems, *Journal of Contaminant Hydrology*, *77*(4), 247-270.

Parks, G. (1965), The isoelectric points of solid oxides, solid hydroxides, and aqueous hydroxo complex systems, *Chemical Reviews*, *65*(2), 177-198.

Powers, S., et al. (1996), Wettability of NAPL-contaminated sands, *Journal of Environmental Engineering*, *122*(10), 889-896.

Ryder, J. (2007), Experimental investigation of the factors affecting the wettability of aquifer materials, Ph.D. thesis, 213 pp, University of Michigan, United States -- Michigan.

Ryder, J., and A. Demond (2008), Wettability hysteresis and its implications for DNAPL source zone distribution, *Journal of Contaminant Hydrology*, *102*(1-2), 39-48.

Singh, U., and G. Uehara (1999), Electrochemistry of the double layer: principles and applications to soils, in *Soil Physical Chemistry*, edited, pp. 1-46, CRC Press, Boca Raton.

Sposito, G. (1989), *The Chemistry of Soils*, Oxford University Press, New York.

Standal, S. H., et al. (1999), Partition coefficients and interfacial activity for polar components in oil/water model systems, *Journal of Colloid and Interface Science*, *212*(1), 33-41.

van Genuchten, M. T. (1980), Closed-form equation for predicting the hydraulic conductivity of unsaturated soils, *Soil Science Society of America Journal*, *44*(5), 892-898.

World Health Organization (2006), Protecting groundwater for health: managing the quality of drinking-water sources, Technical Report, IWA Publishing, London.

Zheng, J., and Powers, SE. (1999), Organic bases in NAPLs and their impact on wettability, *Journal of Contaminant Hydrology*, *39*, 161-181.

Zheng, J., et al. (2001), Asphaltenes from Coal Tar and Creosote: Their Role in Reversing the Wettability of Aquifer Systems, *Journal of Colloid and Interface Science*, *244*(2), 365-371.

Chapter 3
The Wettability of a PCE/Organic Base Mixture on Quartz and Iron Oxide Surfaces

3.1.Introduction

Dense Non-Aqueous Phase Liquids (DNAPL), immiscible liquids heavier than water, released to the subsurface may pose a serious risk to the surrounding environment and populace. Although much effort has been made in recent years to limit the risks associated with DNAPL contaminated sites, a lack of knowledge in several key areas frequently hinders remediation efforts [*National Research Council*, 2005]. One such area is the impact of wettability of DNAPL/water mixtures [*Dwarakanath et al.*, 2002] on DNAPL source zone architecture and remediation efficiency [*Powers et al.*, 1996]. Wettability is defined as the tendency of one fluid to preferentially spread over a solid surface in the presence of another fluid [*National Research Council*, 2005]. For the purposes of this study 'wettability' refers to the contact angle (θ) measured through the aqueous phase, 'advancing contact angle' refers to a Non-Aqueous Phase Liquid (NAPL) advancing over the solid surface and 'receding contact angle' refers to NAPL receding over the solid surface. A system with an advancing contact angle $0^{o}<\theta<70^{o}$ is typically considered water-wetting, $70^{o}<\theta<120^{o}$ is intermediate wetting and $120^{o}<\theta<180^{o}$ is NAPL-wetting [*Powers et al.*, 1996].

The subsurface has been typically assumed to be water-wetting [*Mayer and Hassanizadeh*, 2005; *Mercer and Cohen*, 1990; *Powers et al.*, 1996], where the aqueous phase surrounds the sand grains in the saturated zone filling the smaller pores and pore throats and DNAPL occupies the larger pores and pore bodies [*Mayer and Hassanizadeh*,

2005]. However, intermediate and NAPL-wetting systems can occur in a wide range of sites: petroleum reservoirs may have their wettability altered to increase oil yields [*Mercer and Cohen*, 1990], numerous coal tar and creosote contaminated sites have been identified as NAPL-wetting [*Birak and Miller*, 2009] and both neat solvents [*Ryder and Demond*, 2008] and solvents containing surface active chemicals act as the wetting fluid under certain conditions [*Demond et al.*, 1994; *Harrold et al.*, 2001; *Harrold et al.*, 2005; *Hsu and Demond*, 2007; *Lord et al.*, 2000]. These surface active chemicals are often added to chlorinated solvents to increase their working efficiency or detergency [*Martin and Fulton*, 1958]. Therefore, the assumption of a water-wet system may be inappropriate in these circumstances, with consequences including incorrect dissolution rates predictions - thus the efficiency of remediation efforts may be misestimated [*Bradford et al.*, 2000] - and that fluid distribution and behaviour may be different than expected - and thus remediation techniques such as waterflooding may be much less effective than anticipated.

Considerable work has been completed studying the effect of small concentrations of compounds typically found in the bulk NAPL on wettability [*Buckley and Liu*, 1998; *Demond and Roberts*, 1991; *Demond et al.*, 1994; *Desai et al.*, 1992; *Hsu and Demond*, 2007; *Lord et al.*, 2000; *Zheng and Powers*, 1999]. While the majority of work to-date has studied crude oil/petroleum wettability [*Buckley and Lord*, 2003] the mechanisms of wettability alterations are similar for any multi-component NAPL mixture. The presence of asphaltenes in coal-tars and creosotes has been correlated with NAPL-wetting behaviour [*Zheng et al.*, 2001] in quartz sands. At high ashphaltene concentrations, NAPL-wetting behaviour was a result of asphaltenes precipitating on to the solid surface.

However at low asphaltene concentrations the switch to hydrophobic wettability was linked to acid/base reactions at the soil surface. An electrical charge developed on the soil surface as a result of the reactions and the polar functional group on the asphaltene molecule sorbed to the electrical charge. This acid/base interaction and surface charge development is commonly associated with altering the wettability of DNAPL waste systems.

Zheng and Powers [1999] hypothesized that the presence of organic bases was required to alter wettability in subsurface NAPL/water systems. That study measured the quantity of organic bases present in a variety of real NAPLs and compared their respective wettabilities using the bottle test method described by Powers [1996]. At low pH values, NAPLs with a relatively high concentration of organic bases exhibited non water-wet conditions while the NAPLs with low organic base concentrations did not. At sufficiently low pH values the organic base would become protonated and develop a cationic charge that would sorb to negatively charged surfaces. Soil dominated by quartz would possess a net negative charge above pH 2 [*Sposito*, 1989] and become increasingly negative with increased pH, under these conditions there would be an electrostatic attraction between the surface and the cationic organic base. The pH value at which the soil carries a net neutral charge, pH 2 for quartz, is termed the isoelectric point. Thus wettability alterations would be expected at pH values above the isoelectric point of a solid and below the pH at which the functional groups on organic bases deprotonate and lose their cationic charge [*Zheng and Powers*, 1999].

Other studies have focused specifically on the wettability of chlorinated solvents containing surface active chemicals [*Demond et al.*, 1994; *Desai et al.*, 1992; *Hsu and Demond*, 2007; *Lord et al.*, 1997; *Lord et al.*, 2000]. A wide array of natural and anthropogenic surface active chemicals are present at NAPL impacted sites [*Buckley and Lord*, 2003; *Hsu and Demond*, 2007; *Lord et al.*, 1997; *Lord et al.*, 2005; *Powers et al.*, 1996; *Zheng and Powers*, 1999; *Zheng et al.*, 2001; *Jackson and Dwarakanath*, 1999; *Dou et al.*, 2008]. Lord et al. [2005] measured the advancing and receding contact angles of tetrachloroethylene (PCE) over quartz slides immersed in water. The measured systems contained a set amount of the organic base dodecylamine (DDA), which is predominantly cationic below pH 10.6. The findings from Lord et al. [2005] are consistent with those from Zheng and Powers [1999] and others [*Demond et al.*, 1994; *Desai et al.*, 1992; *Hsu and Demond*, 2007]: wettability alteration is a function of the amount of cationic DDA in aqueous solution and the amount of negative charge on the quartz surface.

However, most of the studies examining the wettability of solvents containing surface active chemicals have used quartz as a solid surface [*Demond et al.*, 1994; *Harrold et al.*, 2001; *Harrold et al.*, 2005; *Hsu and Demond*, 2007; *Lord et al.*, 1997; *Lord et al.*, 2000; *Lord et al.*, 2005; *Powers et al.*, 1996; *Powers and Tamblin*, 1995]. While quartz is a very common subsurface material, other minerals are common and exhibit distinct isoelectric properties from quartz [*Sposito*, 1989] as can be seen in Table 3 which lists some common subsurface minerals and the points of zero charge associated with them. A number of the minerals listed in Table 3 have points of zero charge, also known as the

isoelectric point that are substantially different from quartz. The isoelectric point of mineral surfaces can vary from pH 2 to 10 [*Parks*, 1965].

As pH increases to the isoelectric point of the solid, the net surface charge of the solid surface switches from positive to negative and as pH continues to increase the surface become more negative [*Singh and Uehara*, 1999]. The isoelectric point of quartz is commonly given as pH 2 [*Parks*, 1965]. Hematite and goethite exhibit an isolectric point in the range of 6 to 8, although values as high as pH 9 have been reported [*Parks*, 1965]. Therefore at neutral pH, quartz is expected to exhibit a larger net negative surface charge than iron oxide. Hence, it is anticipated that more DDA, which is positively charged at neutral pH, will adsorb to a quartz surface than an iron oxide surface. The quartz surface is expected to be rendered less water-wetting than the iron oxide surface due to a greater mass of adsorbed DDA. Similar behavior is anticipated with any of the other minerals listed in Table 3 with an isoelectric point higher than quartz. These minerals can have an impact that is disproportionately greater than their percentage of the total soil mass. A single sand grain will form a pore wall for several pores and can thus affect a water drainage or imbition behavior for numerous pores. Bauters et al. [2000] calculated that if only 3.1% of sand grains were hydrophobic then up to 37% of the pore spaces would have a pore wall that is hydrophobic.

Table 3. Common Soil Minerals[1] and Points of Zero Charge

Name	Ubiquity in Soils	Environment	Point of Zero Charge
Quartz	Ubiquitous	Nearly all soils and parent materials	2[2]
Hematite and Goethite	Ubiquitous	Well-drained, near surface soil	6-10[3]
Feldspars	Rare to common	Wide variety of igneous and metamorphic rocks	2-2.4[1]
Gibbsite	Common	Old, stable soils or feldspar pseudomorphs	8-9[1]
Kaolinite	Ubiquitous	Desilication of 2:1 lays/feldspathic	4-5[1]
Calcite	Common	Arid soils	9.5[1]
Hydroxy-interlayered vermiculite	Ubiquitous	Acid, highly weathered soil surface horizons	P[1,4]
Muscovite	Common	Granitic and high-grade metamorphic rocks	P[1,4]

[1][*Feldman et al.*, 2008]
[2][*Cornell*, 2003]
[3][*Parks*, 1965]
[4] Indicates that the soil maintains a permanent negative charge at all pH values

The Cassie equation [*Cassie*, 1948] illustrates the dependence of the apparent contact angle of a mixture of sands with different wettabilities on the surface area of each sand fraction. This equation is given as:

$$Cos(\theta) = f_1 \cos(\theta_1) + f_2 \cos(\theta_2) + \ldots f_i \cos(\theta_i) \qquad [2\text{-}10]$$

Where f_i represents the surface area fraction for a certain material and θ_i is the contact angle on that material. A small amount of mineral with a high surface area may have a disproportionate impact on the apparent contact angle of the sand. Thus even minor

variability in subsurface minerals may have a large impact on DNAPL distribution and wettability in the subsurface.

Despite the presence of surfactant additives in chlorinated solvents and the important role isoelectric properties play in determining NAPL wettability, there has been almost no work examining the wettability of surfactant/chlorinated solvent mixtures on non-quartz surfaces. The effect of surfactants and changing contact angles have been demonstrated on quartz sands using various NAPL/surfactant systems [*Demond et al.*, 1994; *Desai et al.*, 1992; *Hsu and Demond*, 2007; *Lord et al.*, 2005; *Lord et al.*, 2000] but still relatively little is known about how a heterogeneous soil containing more than one mineral type can affect subsurface wettability in the presence of a DNAPL/surfactant mixture. The impact of mineral variability on neat solvent wettability has already been demonstrated [*Ryder et al.*, 2008] and it was shown that the hysteresis of neat solvents varied with the oxygen content on a mineral surface [*Ryder et al.*, 2008] however the role of surfactants was outside the scope of that study.

As shown in Table 3 the isoelectric point of subsurface minerals can vary from pH 2 to 10 and a wide array of surface active chemicals can be found in the subsurface at NAPL contaminated sites, both natural and anthropogenic [*Buckley and Lord*, 2003; *Hsu and Demond*, 2007; *Lord et al.*, 1997; *Lord et al.*, 2005; *Powers et al.*, 1996; *Zheng and Powers*, 1999; *Zheng et al.*, 2001]. So to develop a better conceptual model of DNAPL in the subsurface the interactions between surfactants, isoelectric point and wettability needs to be understood.

The goal of this study was to determine the impact of DNAPL composition on the wettability alterations of quartz and iron oxide surfaces and to assess the impact of wettability on DNAPL migration in soils containing these minerals. In particular, the role of mineral isoelectric point and surfactant properties on wettability alterations was examined for PCE containing the cationic surfactant DDA. This study first determined the effect of pH on advancing and receding contact angles for the fluid pair PCE/water on both quartz and iron oxide surfaces in the presence of DDA. Second, it quantified PCE/water primary drainage capillary pressure-saturation (P_c-S) relationships for quartz and iron oxide sands in the presence of DDA at both low and neutral pH, which provide an important contrast in mineral surface charges. Third, this study assessed the migration behaviour of PCE/DDA in these sands at the two pH conditions in a small two-dimensional flow cell. This methodology provides the means to link wettability properties at the pore (contact angle) and representative elementary volume (REV) scales (P_c-S functions) to DNAPL behaviour in porous media for these unexplored solid-fluid-fluid systems.

3.2.Materials and Methodology

3.2.1. Materials

The aqueous phase used throughout this study was distilled, deionized water (Milli-Q filters, Millipore). Aqueous phase ionic strength was controlled with NaCl (>99.5%) (Sigma-Aldrich). The target aqueous phase pH was achieved using either HCl (Analytical Reagent grade, EML) or NaOH (reagent grade pellets, Sigma-Aldrich). The DNAPL employed was PCE (>99% purity, Acros Organics) dyed with Oil-Red-O (Fluka) at 0.01g/L. Oil-Red-O was selected as it does not significantly impact interfacial properties at the concentration employed in this study [*Jeong et al.*, 2002; *Tuck et al.*, 2003]. Dodecylamine (DDA) (98% purity, Acros Organics) was selected as the surface active chemical to facilitate comparison with literature studies [*Hsu and Demond*, 2007; *Lord et al.*, 2000; *Lord et al.*, 2005]. DDA is a weak organic base in solution with a pK_a of 10.6 [*Lord*, 2005]. The aqueous solubility of DDA depends heavily upon its speciation, cationic DDA has a solubility of $1x10^{-3}$M and the neutral form has a much lower solubility of $2x10^{-4}$M [*Lord*, 1999]. The distribution of DDA between aqueous and non-aqueous phases was also found to be heavily pH dependant [*Lord*, 1999]. At low pH values the cationic DDA would partition into the aqueous phase. At higher pH values where DDA was predominantly neutral it would partition out of the aqueous and back into the NAPL [*Lord*, 1999]. pH values were measured with a pH meter (Thermo-Scientific) accurate to +/- 0.002 that was calibrated before each use with a three-point calibration curve.

Iron oxide was chosen as the non-quartz surface in this study because of its ubiquity in the ground and the isoelectric point it shares with a number of other common subsurface

minerals. So contact angles were measured on smooth quartz and iron oxide plates (Alfa Aesar) which, for the purpose of ensuring oxidation, were first immersed in a pH 13 solution and then heat treated at 500°C for 12 hours. XPS analysis of the iron plates revealed the presence of magnetite and hematite. The surface of the iron plate had visible heterogeneities implying that the oxide types were not homogeneous across the surface.

Sandbox and multi-step outflow experiments were performed with F-70 silica sand (Opta Minerals). Iron oxide-coated F-70 sand was created using an established procedure [*Johnson et al.*, 1996]. The silica sand was thoroughly cleaned followed by overnight immersion in a 0.72M $FeCl_3$, pH 6.5 solution, then dried and heated overnight at 700°C. XPS analysis revealed that the sand surface was predominantly hematite and goethite. Based on values in the literature the isoelectric points for the iron plate and iron-coated sand were estimated to be between pH 6.5 and 8 in contrast to pH 2 for the quartz plate and quartz sand [*Cornell*, 2003; *Parks*, 1965].

3.2.2. Cleaning Procedures

Particular attention was devoted to ensuring that all instruments, glassware and sand were free of impurities, particularly surfactant impurities that could affect interfacial properties. All glassware and instruments were cleaned prior to use with an established procedure [Lord et al., 2000]: immersion overnight in a 2% Micro-90 cleaning solution (International Products Corporation), rinsing with Milli-Q water, rinsing with reagent grade acetone (Caledon), rinsing with Milli-Q water, rinsing with 0.1N HCl, rinsing with

Milli-Q water, rinsing with 0.1N NaOH, and final rinsing with Milli-Q water. The quartz plates were cleaned in a similar manner and, in addition, were soaked in 12M HCl for 20 minutes and then rinsed with Milli-Q water. Metal columns, needle tips and iron plates were rinsed thoroughly with acetone and Milli-Q water. Sands were cleaned by soaking in 0.1M Sodium Dithionite (Mallinckrodt) solution for two hours, rinsed thoroughly with water, soaked in 3% hydrogen peroxide solution (Mallinckrodt) for 3 hours, rinsed with Milli-Q water, soaked in acidic water overnight and dried at 30-40°C [Johnson et al., 1996]. At this point the sand was either used as is for quartz sand experiments or treated to yield an iron oxide coating.

NAPL/Water Systems were created using the same procedure for each set of experiments. DDA was added directly into the PCE phase in a flask containing a 1:6.3 volumetric ratio of PCE to water at $[DDA]_T$=0.0027M. The pH of the aqueous phase would then control the speciation and distribution of DDA between the two phases [Lord et al., 2000]. $[DDA]_T$ is the amount of DDA in the system normalized to the volume of the aqueous phase and given by the formula:

$$[DDA]_T = \frac{[DDA]_{aq} V_{aq} + [DDA]_{org} V_{org}}{V_{aq}} \qquad [3\text{-}1]$$

The systems were titrated to their target pH by adding 0.1N HCl to the solution followed by equilibration on a vibrating table for 24 hours and repeating until the desired pH was achieved. Once the desired pH was achieved, the chemical systems were let to sit for at least 24 hours before usage to ensure equilibration.

3.2.3. Interfacial Tension and Contact Angle Measurements

Interfacial tensions (pendant drop method with equilibrated water/PCE/DDA at target pH) and contact angles were measured using an Axisymmetric Drop-Shape Analysis system (First Ten Angstroms) [*Lord et al.*, 2000]. Slides were equilibrated in the aqueous phase of the PCE/water systems previously created for a minimum of 72 hours. A syringe containing 5 μL of PCE was controlled by a stepping motor that would slowly expel PCE onto the slide surface for advancing contact angle measurements. The stepping motor would reverse after 5 μL and draw the PCE back up into the syringe for the receding contact angle. For contact angle measurements, the needle tip remained just above the slide surface and inside the PCE drop to ensure stable, repeatable contact angle measurements. Digital photographs of the PCE droplet were recorded every 0.1 seconds as the droplet slowly advanced and receded over the slide. Computer software would then fit a contact angle to the droplet and this value was recorded as either the advancing or receding contact angle. At least 10 measurements were taken at different locations on the surface for each target pH value for each material; these provide confidence intervals on the spatial variability of contact angle for each surface as a function of pH. To avoid distorting the shape of the droplet due to gravity the volume of the droplet never exceeded 5 μL.

Statistically, the advancing and receding contact angle values shown represent the mean of all contact angles measured at a single pH and are accompanied by the calculated 95% confidence interval. The calculated mean may incorporate multiple PCE droplets at a single pH. Interfacial tension values are reported as a mean value in pH intervals of 0.5

accompanied by the 95% confidence interval if more than 3 measurements were recorded in that 0.5 pH interval.

3.2.4. Capillary Pressure-Saturation Experiments

PCE/water primary P_c-S relationships were quantified for iron oxide and quartz sands at an aqueous pH of 6.3 and 3.4±0.2 using the multistep outflow approach followed by O'Carroll et al. [2005b]. This method, instead of stepwise measuring P_c-S data pairs, employs a multi-phase flow simulator to fit a P_c-S relationship to outflow results from a column experiment in which NAPL displaces water from a volume of sand over several discrete pressure steps in the NAPL phase. The experimental setup for the experiment can be seen in Appendix A. The multistep outflow approach was chosen because reliable P_c-S curves (i.e., equivalent to those from static experiments) can be obtained relatively quickly compared to the static method of determining P_c-S curves [O'Carroll et al., 2005b].

Table 4 provides an overview of the conditions at which the P_c-S experiments were performed. The P_c-S experiment conducted in the absence of DDA provided a validation of the method (Appendix B). Aluminum columns (length = 9.62/10.12cm, ID = 5.07cm) were dry packed with F-70 quartz or iron oxide sands in 1-2cm lifts following the procedure of O'Carroll et al. [2004]. The column was then flushed with CO_2 for approximately 1 hour to displace all the air. The column was saturated with de-aired water at a rate of approximately 3mL/min for 2 hours and left overnight. Saturated permeability was determined using the constant head method. A water-wet nylon membrane (0.2μm pore size, Pall Corporation) was then placed at the top end of the

column to prevent NAPL outflow which would have interfered with the mass balance. A constant-head test was performed again with the membrane in place to measure the permeability of the membrane. The column was then flushed with the equilibrated aqueous solution at a rate of approximately 2mL/min until the influent and effluent aqueous phase surface tensions were within 1 mN/m.

Table 4: Capillary Pressure-Saturation Experiments

pH	Sand Type	Porosity	IFT (mN/m)
NA	Quartz, no DDA present	0.29	47.1
3.2	Quartz	0.34	6.99
3.6	Iron oxide	0.34	6.06
6.3	Quartz	0.34	14.4
6.3	Iron oxide	0.33	14.4

The bottom of the column was connected to a constant pressure PCE reservoir (ID = 10.05cm) [*O'Carroll et al.*, 2005b] which was controlled by an air pressure/vacuum system. The pressure in the water phase was held constant by fixing the height of the outflow tube. The outflow was collected in a reservoir and measured with a digital balance (Mettler-toledo). The water reservoir was partially covered in parafilm to minimize evaporation. PCE and aqueous phase pressures were tracked using FP2000 pressure transducers (Honeywell) and were recorded digitally using a CR7 datalogger (Campbell Scientific). See Appendix A for a diagram of the apparatus. The air pressure

attached to the PCE reservoir was increased incrementally (4-8 steps per experiment) at intervals of 3 to 8 hours or whenever the outflow had approached equilibrium.

At the completion of the P_c-S experiments, van-Genuchten P_c-S model parameters α, n and S_{wr} [*van Genuchten*, 1980] were fit using an inverse modeling approach [*O'Carroll et al.*, 2005b]. P_c-S curves were then plotted using the van-Genuchten equation (equation [3-2])and the fit parameters α, n and S_{wr} .

$$P_c = \frac{\left[S_e^{\frac{-1}{m}} - 1\right]^{\frac{1}{n}}}{\alpha} \qquad [3\text{-}2]$$

Where m is assumed to be 1-1/n. S_e is the effective saturation and is given as:

$$S_e = \frac{S_w - S_{wr}}{1 - S_{wr}} \qquad [3\text{-}3]$$

Where S_w is the water saturation and S_{wr} is the residual water saturation fit by the model. The resulting curves were scaled to one another using a modified Leverett scaling technique that has been previously employed to scale P_c-S curves with water-wet and NAPL-wet sands [*Demond et al.*, 1994; *Desai et al.*, 1992]:

$$P_{c2}(S_e)_2 = P_{c1}(S_e)_1 \frac{(\gamma_2 \cos\theta_r Z(\theta))_2}{(\gamma_1 \cos\theta_r Z(\theta))_1} \qquad [3\text{-}4]$$

Where P_{c1} and P_{c2} are the capillary pressures being scaled, S_{e1} and S_{e2} are the effective saturations for the capillary pressures and γ_1 and γ_2 are the interfacial tensions for each system. The $Z(\theta)$ and θ_r terms were introduced by Melrose [1965] and Morrow [1975], respectively, to better account for actual pore geometry. Contact angle θ_r is referred to in

this study as the operative contact angle observed directly in a soil matrix. The operative contact angle relationship developed by Morrow [1975] is:

$$0^o < \theta_{int} < 21.6^o \quad \theta_r = 0 \qquad [3\text{-}5]$$

$$21.6^o < \theta_{int} < 87.6^o \quad \theta_r = 0.5\exp(0.05\theta_{int}) - 1.5 \qquad [3\text{-}6]$$

Where θ_{int} is the intrinsic contact angle measured on smooth slides. Equation [3-4] was used to fit θ_r to any Pc-S curve with an intrinsic contact angle outside of the range specified in equations [3-5] and [3-6] . Equations [3-5] and [3-6] were applied to three P_c-S experiments; the pH 3.2/3.6 quartz and iron oxide experiments and the pH 6.3 iron oxide experiment. The contact angle measured on quartz at pH 6.3 was outside the applicable range [Morrow, 1975]; thus, the operative contact angle for that experiment was determined by scaling Equation [3-4] via the operative contact angle to minimize the difference between the quartz and iron oxide curves at pH 6.3.

The multiphase flow simulator was employed to fit the van-Genuchten parameters by minimizing the squared difference between the observed outflow and simulated outflow from the column using a Levenberg-Marquardt algorithm. It should be noted that dynamic effects in capillary pressure were not fit since the goal of this study was to estimate the capillary pressure-saturation relationship. The study of O'Carroll et al. [2005b] found that the inclusion of dynamic effects in capillary pressure in the governing phase mass balance equations of the numerical simulator was not required to achieve good estimates of capillary pressure/saturation relationships.

3.2.5. Flow Cell Experiments

Flow cell experiments were run at pH 3.5 and pH 6.8 in a 5 cm x 5 cm x 1 cm thick aluminum flow cell with glass on the front and back face facilitating visualization via light transmission. This cell was previously employed for multiphase flow research [*Gerhard and Kueper*, 2003] and was adapted for this work. The packing and saturation procedure was similar to that employed for the P_c-S experiments. However, in this case a specific heterogeneous packing was employed (Figure 5) to allow direct comparison of DNAPL migration into both sands under identical boundary pressures. The packing arrangement chosen, a T-shaped iron oxide block surrounded by a quartz U, was to keep the area of interest, the iron oxide heterogeneity, in the middle of the flow cell away from potential wall effects. A layer of iron oxide sand was emplaced at the top of the flow cell to provide a hydrophilic NAPL barrier similar to the nylon membrane used in the P_c-S experiments. It was expected that the PCE behaviour observed in the flow cell could be predicted based on the contact angle and P_c-S relationships. Table 5 lists an overview of the conditions at which the flow cell experiments were completed.

Table 5: Flow Cell Experimental Conditions

pH	IFT (mN/m)	Porosity
3.5	9.9	0.31
6.8	19	0.33

The chemical systems used were the same as those in the P_c-S experiments and are described in section 3.2.3. After packing and saturation were complete, the cell was

flushed with aqueous solution that had been equilibrating with the PCE/DDA mixture. Flushing continued until the influent and effluent surface tensions of the aqueous phase were within ±1 mN/m.

The bottom of the sandbox was attached to a PCE reservoir that could be raised to control the DNAPL pressure. The top of the sandbox was connected to a tube terminating at a set height and open to the atmosphere to control the aqueous phase pressure. See Appendix A for a diagram of the apparatus. The height of the PCE reservoir was increased in approximately 0.5 cm increments and the fluids in the sandbox were allowed to reach equilibrium between each migration step. The system was considered to have reached equilibrium if 30 minutes passed with no additional advancement of the NAPL/water interface. At equilibrium, the controlling capillary pressure was estimated by assuming hydrostatic conditions in the flow cell. Each image was analyzed afterwards in Matlab to examine the physical distribution of PCE throughout the flow cell.

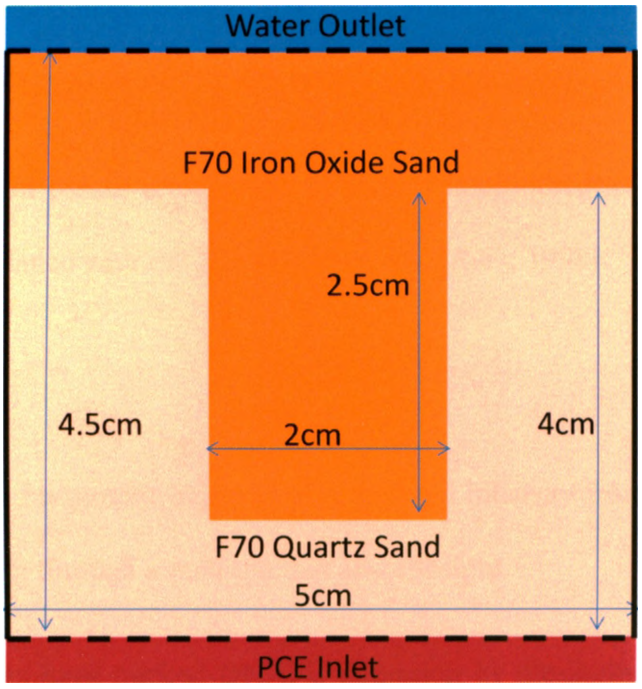

Figure 5: The packing configuration of the flow cell. A T-shaped iron oxide heterogeneity was packed surrounded by a bed of quartz sand.

Light transmission visualization (LTV) was used due to its ability to accurately track multiphase flow in a two-dimensional porous media environment [*Niemet and Selker*, 2001]. A digital camera (Nikon D80 with Nikkor 35-75mm lens) was automated by commercial computer software (Nikon Camera Control Pro) to photograph the cell at programmed intervals. A remotely controlled camera flash (Nikon SB800) was employed as the light source at the back of the cell, and was triggered automatically in tandem with each photograph. In this manner the image acquired integrated information on the pore fluids across the sand pack thickness. This setup had the added advantage of avoiding the temperature change that often results from a typical light bank. Camera and flash controls were kept consistent for the two experiments. No light diffuser was used on the flash and there was no post-processing of the images for exposure or flash compensation.

The experiment took place in a dark room to eliminate variations in background light and the flash was shuttered so that all of the light passed through the apparatus.

As light passes through the system, it is absorbed as a function of NAPL saturation in accordance with the Beer-Lambert law [*Ryer*, 1998]:

$$A = -\log_{10}\frac{I}{I_o} \qquad [3\text{-}7]$$

I_o and I represent, respectively, the light intensity from the camera flash before and after passing through a medium that absorbs light.

Studies have tracked DNAPL migration by measuring changes in hue [*Darnault et al.*, 1998; *O'Carroll et al.*, 2004], changes in colour saturation [*Gerhard and Kueper*, 2003] and changes in light intensity [*Bob et al.*, 2008; *McNeil et al.*, 2006; *Niemet and Selker*, 2001; *Wang et al.*, 2008]. In this work, the sRGB colorspace digital images were converted to light intensity (I) using the equation [*Stokes*, 1996]:

$$I = 0.2126R + 0.7152G + 0.0722B \qquad [3\text{-}7]$$

The application of the Beer-Lambert law allowed for a pixel-by-pixel analysis of yes/no PCE presence throughout the flow cell. The Beer-Lambert law was applied by calculating three different values of absorption (A) for each image: A_{sand} is the absorption of the sandpack when saturated with water, A_{PCE} is the adsorption constant for the pure PCE phase dyed with Oil-Red-O and $A_{PCE,sand}$ is the adsorption coefficient that was used to predict the effluent light intensity for a pixel containing both sand and PCE.

Absorbance values for each sand pixel were calculated and summed with the absorbance values measured for PCE to obtain $A_{PCE,sand}$. Using the calculated $A_{PCE,sand}$ value it was possible to predict the drop in light intensity associated with the presence of PCE for each pixel in the flow cell. In this work, it was not possible to quantify DNAPL saturations due to side reservoirs (associated with the cell's previous use) which did not affect the equilibrium heights of PCE in the flow cell, also allowed for the measurement of PCE's light absorbance but interfered with the mass balance needed for determining saturation. As proven in other studies employing multiphase flow tracking in heterogeneous porous media [*Grant et al.*, 2007], the DNAPL/water interface can be accurately tracked in time without determining specific saturations at every location.

3.3.Results and Discussion

3.3.1. Contact Angle and Interfacial Tension

Contact angles were measured on smooth quartz and iron oxide slides for $3.2 < pH < 7.5$ values and $[DDA]_T$ =0.0027M to assess the impact of surface charge and DDA on wettability. Contact angles were not measured above a pH of 7.5 because DDA begins partitioning back into the PCE phase at that pH. The pH range captures the majority of difference between the isoelectric points of quartz (pH 2) and iron oxide (pH 6 - 9) [*Parks*, 1965]. Figure 6 provides an example ADSA measurement on the two solids at pH 6.5. At pH 6.5, the quartz surface was highly hydrophobic while the iron oxide plate remained strongly hydrophilic (Figure 6). Measurements of advancing contact angle at a variety of locations on both the quartz and iron oxide coated surfaces yielded consistent results. The differences observed at pH 6.5 between the quartz and iron oxide plates are hypothesized to be due to surface charge contrast.

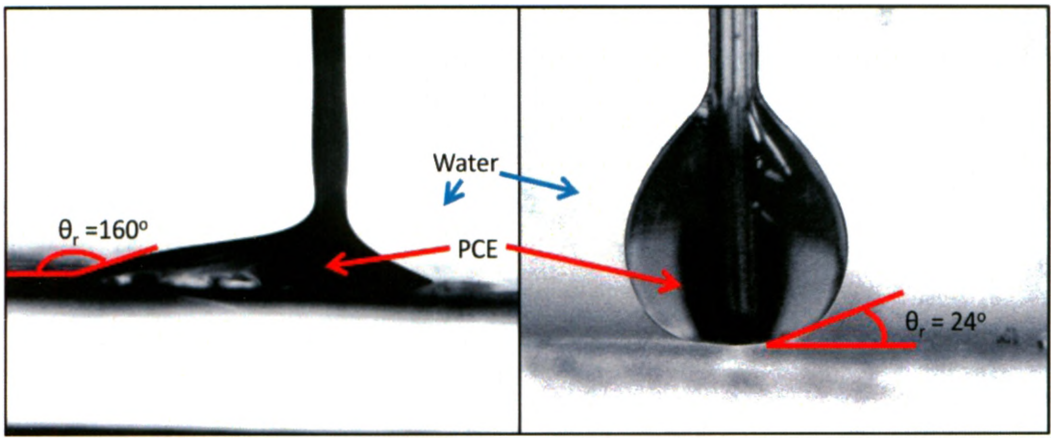

Figure 6: PCE droplets advancing over quartz (left image) and iron oxide surfaces (right image) immersed in water at pH 6.5. The needle tip was left in the PCE droplet during imaging. $[DDA]_T$ =0.0027M

The PCE advancing contact angle on quartz was observed to be a strong function of pH at $[DDA]_T$=0.0027M (Figure 7). At low pH, the quartz remained strongly hydrophilic with an average value of 24° at pH 3.7. Due to the small net negative surface charge of quartz at low pH, little DDA sorbs on to the quartz surface despite an abundance of cationic DDA in solution. With increasing pH, the quartz surface became NAPL-wetting with a maximum contact angle of 158° measured at pH 6.2 (Figure 7). This is likely an optimal system point where the cationic DDA concentration is at solubility in the aqueous phase ($1x10^{-3}$M) and the quartz has a strong net negative charge. At pH above 6.5, contact angles are observed to decrease into the intermediate wettability range and variability across the surface increases significantly. It is hypothesized that this is because the DDA partitions back into the organic phase at these pH values, and the reduced aqueous phase DDA concentration results in less coverage of DDA on the plate and this causes smaller, more irregular contact angles. Lord et al. [2000] observed more scatter in their contact angle measurements across all pH values, likely due to the lower DDA concentration employed in their study ($[DDA]_T$ = 0.001). Overall, the advancing contact angle trends measured on the quartz plate are consistent with previous studies involving DDA [*Hsu and Demond*, 2007; *Lord et al.*, 2000; *Lord et al.*, 2005].

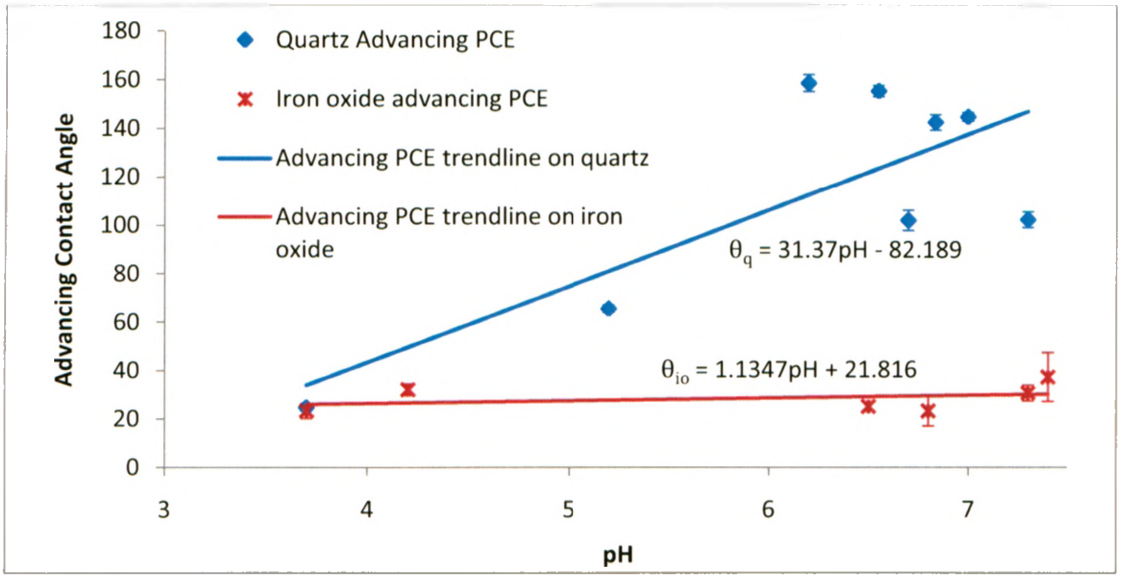

Figure 7: Advancing contact angle versus pH for PCE on quartz and iron oxide surfaces as measured through the water phase with $[DDA]_T$ =0.0027M. Each symbol represents the mean of at least 10 measurements and is presented with its associated 95% confidence interval (where it is not visible, the interval is smaller than the symbol dimensions). Best fit linear regression trendlines for contact angles measured on quartz and iron oxides are overlain.

In contrast to the results for quartz, PCE advancing contact angles on the iron oxide surface suggest that the surface is hydrophilic throughout the entire pH range (Figure 7) in the presence of DDA. In this pH range both the iron oxide plate and DDA are positively charged resulting in no sorption of DDA on the plate. The advancing contact angles on quartz and iron oxide plates were significantly different over the majority of the pH range. The maximum difference measured in the advancing contact angles was 130° at pH 6.5, with the iron oxide surface being hydrophilic (25°) while the quartz surface was hydrophobic (155°) under identical conditions. The data in Figure 7 suggests the common assumption that subsurface wettability is homogeneous [*Powers et al.*, 1996] may not apply to iron oxide-coated materials. It should be noted that error bars

representing 95% confidence intervals are included for each point on Figure 7 and 10 and may be difficult to see because of the consistency of the measurements. Also, the iron oxide contact angles measured in the presence of DDA were similar to the contact angle of a pure PCE/water/iron oxide slide.

Because entry pressure is dependent upon the cosine of the contact angle (equation [2-3b]), cos(θ) was plotted versus pH to ensure the differences in contact angle between quartz and iron oxide surfaces manifest as differences in cos(θ). Plotting cos(θ) versus pH for both iron oxide and quartz surfaces (Figure 8) yielded similar trends to Figure 7. The cos(θ) trend for iron oxide suggests that little to no reduction in displacement pressure due to wettability will occur for iron oxide sands whereas the quartz cos(θ) trend suggests reductions in displacement pressure due to wettability at neutral pH values. θ values above 90^{o} result in a negative cos(θ) (equation [2-3b]) which implies spontaneous imbibition of NAPL into sand. However, as discussed in equations [3-5] and [3-6] the intrinsic contact angle measured on a smooth plate is not identical to operative contact angles in porous media.

The interfacial tensions of the employed PCE/water/DDA systems were observed to be dependent upon pH (Figure 9). The pure PCE/water IFT was measured to be 47 mN/m. Lord et al. [2000] found that as pH reduced, more cationic DDA would align itself at the NAPL/water interface, resulting in reduced IFT values. In that study, with a DDA concentration 2.7 times less than this study, IFT reached a minimum of 20 dynes/cm at pH < 5. In this study, IFT decreased rapidly from a mean of 23 mN/m at pH 7.2 to 13 mN/m at pH 6.3 (Figure 9). This sharp decrease occurred due to the partitioning of

cationic DDA from the organic phase into the aqueous phase until the aqueous phase reached solubility. IFT decreased more slowly below pH 6.3 to a minimum mean of 6.5 mN/m at pH 3.2 (Figure 9). While the cationic DDA has reached aqueous solubility at pH 6.3 there is still a tendency for DDA remaining in the organic phase to continue accumulating at the PCE/water interface.

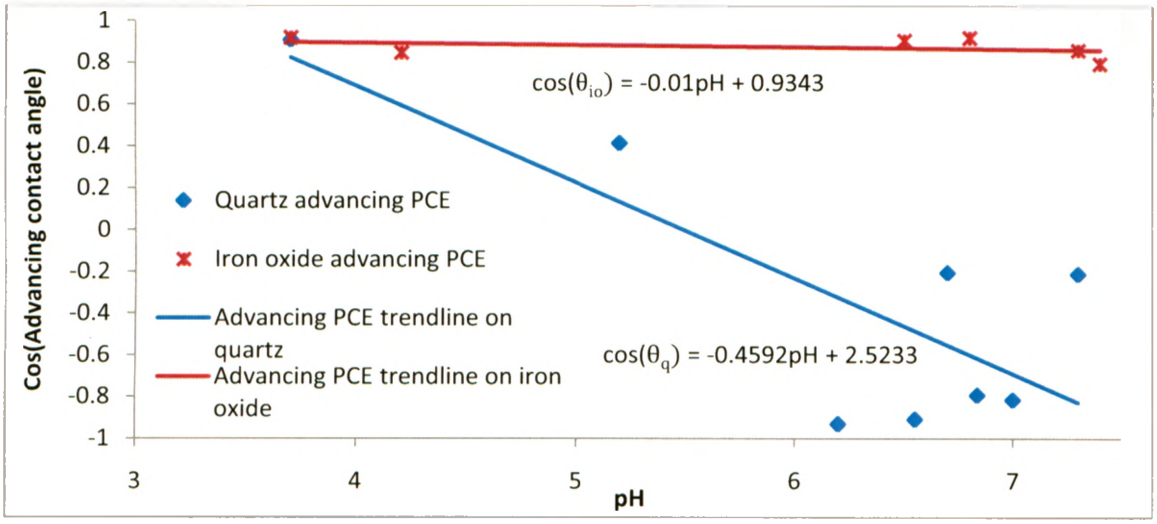

Figure 8: Advancing cos(θ) versus pH for PCE on quartz and iron oxide surfaces as measured through the water phase with $[DDA]_T$ =0.0027M. Each symbol represents the mean of at least 10 measurements. Best fit linear regression trendlines for contact angles measured on quartz and iron oxides are overlain.

PCE receding contact angles were also quantified over the same pH range (Figure 10). Above pH 6, quartz was so hydrophobic that PCE would not recede whatsoever; instead a thin PCE film remained on the quartz surface after the droplet was retracted. Therefore, above pH 6 the receding contact angle on quartz is reported as 180°.

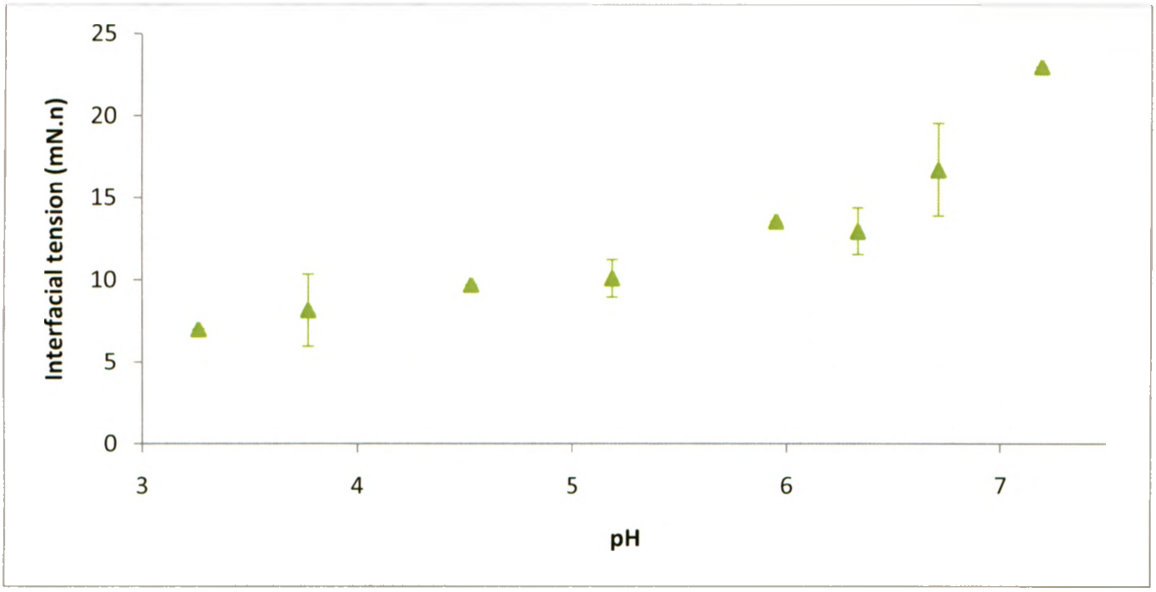

Figure 9: Averaged interfacial tension measurements versus pH for PCE/water/DDA with $[DDA]_T$ =0.0027M.

Hysteresis of contact angle was observed over the evaluated pH range on the quartz surface with the receding always greater than the advancing contact angle (Figures 7 and 10). On the iron oxide surface, very little hysteresis was observed in contact angle in the pH range 3.7-6.3. However, receding contact angle increases sharply from 27° at pH 6.5 to 126° at pH 6.8 as the iron oxide transitions through the isoelectric point in this range and the surface begins to develop a negative charge (Figure 10). At pH 7.4 a thin film of PCE remained on the iron oxide surface, representing strong lipophilic behaviour similar to that observed at pH 6 for quartz. While the magnitude of the hysteresis (ranged from 24° to 77°) was expected for quartz [*Desai et al.*, 1992], the even greater contact angle hysteresis (142°) for iron oxide has not been previously reported. This suggests that the order of fluid contact is more important on an iron oxide surface at neutral pH than a quartz surface.

Given that the contact angles on both quartz and iron oxide plates were measured under identical environmental conditions, the observed differences in wetting behaviour is expected to be due to the differences in the isoelectric point of the surfaces, and the corresponding different affinity of the DDA for those surfaces. If this hypothesis is valid, primary drainage P_c-S relationships in quartz and iron oxide-coated sands using a single DNAPL/water/DDA system would be different at neutral pH and similar at low pH.

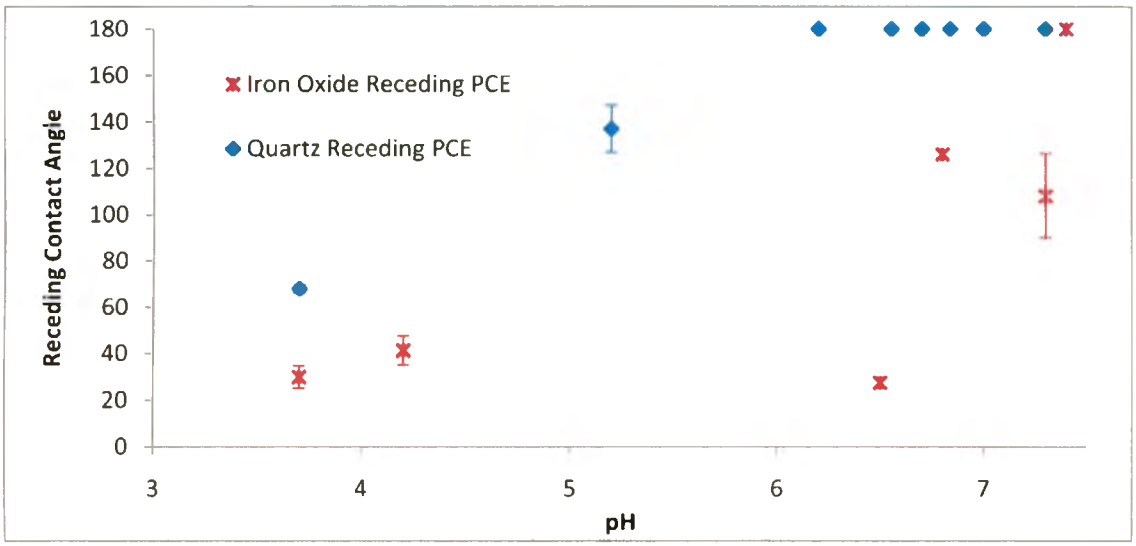

Figure 10: Contact angles of PCE receding over quartz and iron oxide surfaces as measured through the water phase as a function of pH. [DDA]T =0.0027M. Where possible, error bars representing 95% confidence intervals are shown.

3.3.2. Capillary Pressure-Saturation

Aqueous phase/PCE/DDA ($[DDA]_T$ =0.0027M) P_c-S relationships were quantified for both iron oxide and quartz sand at pH 3.4 ± 0.2 and pH 6.3 using a multistep outflow approach [*O'Carroll et al.*, 2005b]. Figure 11 presents the primary drainage P_c-S relationships obtained for the quartz and iron oxide sands at pH 6.3. Capillary pressures were, on average, larger by approximately a factor of 2 in the iron oxide system than the quartz system. The iron oxide-coated sand exhibited higher capillary pressures than the uncoated sand by 4-5cm water over the majority of the water saturation range. This significant difference is consistent with the observed difference in advancing contact angles at pH 6.3: larger advancing contact angle (quartz) - and, thus, less water wetting - correlates to lower primary drainage P_c-S.

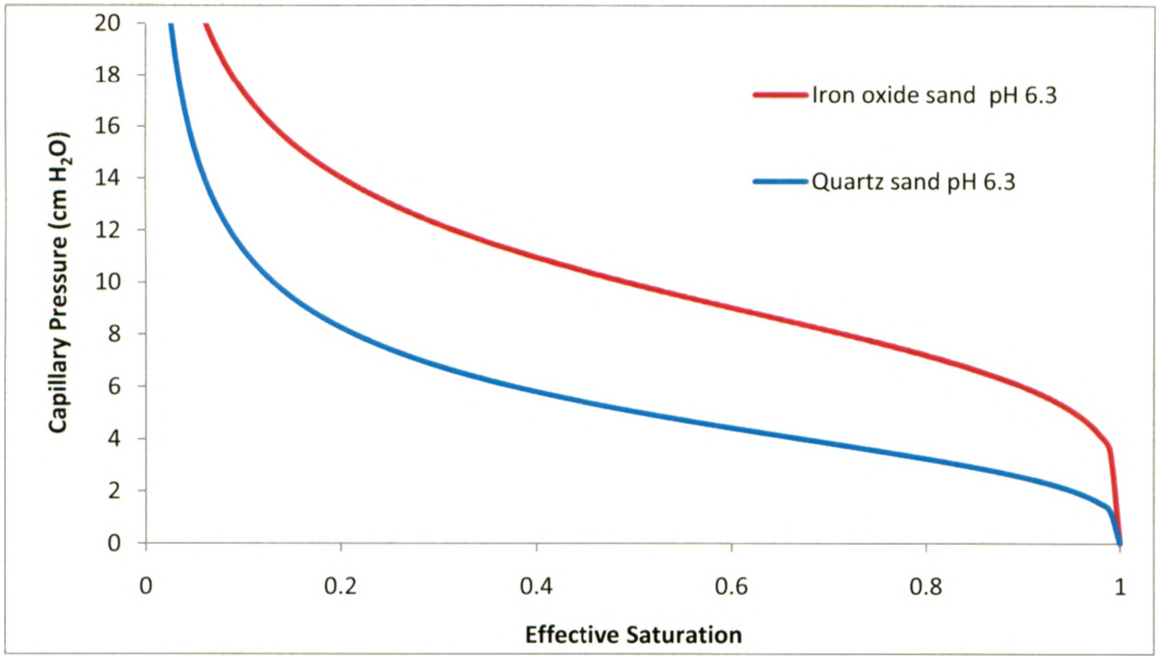

Figure 11: Pc-S relationships for quartz and iron oxide sands at a pH of 6.3 where $[DDA]_T$ =0.0027M.

In contrast to Figure 11, Figure 12 demonstrates that the P_c-S relationships obtained for the quartz and iron oxide systems at pH 3.4 ± 0.2 are similar. This too is consistent with the contact angle measurements, which were similar for quartz and iron oxide at low pH. Figures 9 and 10 underscore that the mineralogical wettability differences observed at the pore scale manifest in contrasting functional differences at the REV scale.

Table 6 lists the van Genuchten parameters fit for the 4 P_c-S experiments completed (corresponding water outflow/pressure data is attached in Appendix B). The fit parameter α varies directly with wettability and IFT. Increases in both the contact angle and the IFT will increase the fit parameter α. At pH 6.3 the two P_c-S experiments were run at the same IFT, but have different fit α values. This suggests a difference in the wettability of the two sands used at that pH. For the two pH 3.2/3.6 P_c-S experiments the α values were similar; this indicates that the wettabilities of the two sands were the same at that pH.

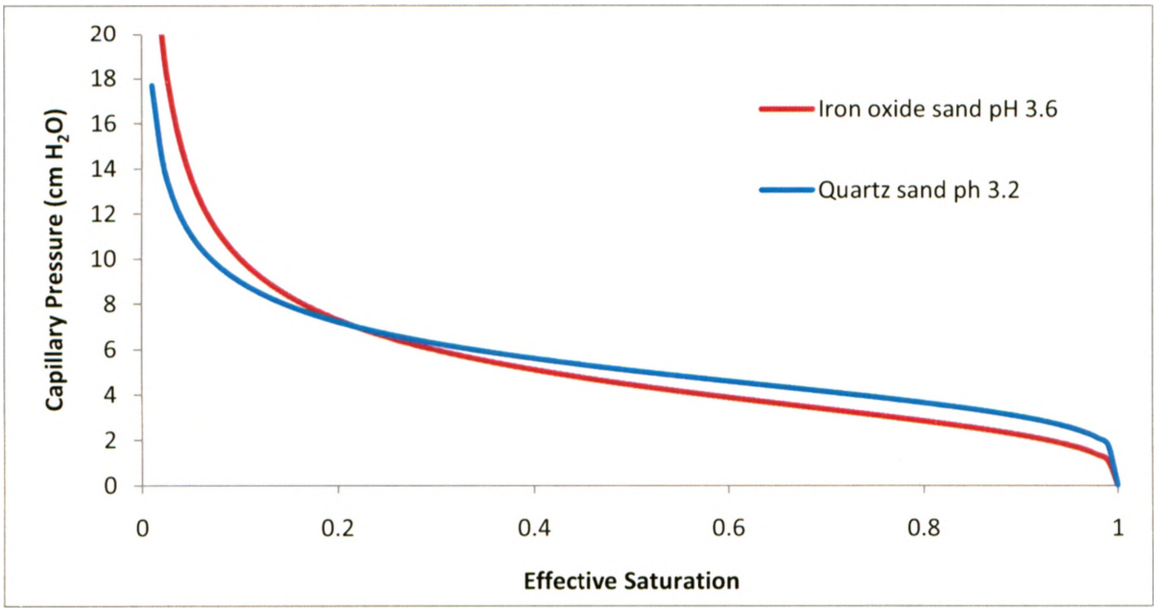

Figure 12: P_c-S relationships for quartz and iron oxide sands at a pH of 3.2 and 3.6 respectively where [DDA]T =0.0027M.

Table 6: Best-Fit Van Genuchten Parameters for P_c-S Experiments

pH	Sand Type	α (1/cm)	n
3.2	Quartz	0.22	4.5
3.6	Iron Oxide	0.26	3.4
6.3	Quartz	0.23	3.4
6.3	Iron Oxide	0.11	4.5

The wettability of the quartz and iron oxide sands was quantified by calculating an operative contact angle for each P_c-S experiment.

Table 7 lists the parameters used to scale each curve using equation [3-4] The operative contact angle of 64° was fit to the pH 6.3 quartz P_c-S curve, while the other three operative contact angles were determined directly, since they were within the appliacable range of Equations 3-5 and 3-6... Figure 13 illustrates the P_c-S curves scaled to the iron oxide pH 6.3 P_c-S curve. It is worth noting that the IFT values used to scale are not the average values seen in Figure 9 but the IFT values that were directly measured for each P_c-S experiment.

Table 7: IFT, Intrinsic and Operative Contact Angles for P_c-S Experiments

pH	Sand Type	Interfacial Tension (mN/m)	Intrinsic Contact Angle (°)	Operative Contact Angle(°)	Curvature Correction
3.2	Quartz	6.9	23	0	0.938
3.6	Iron Oxide	6.1	24	0	0.938
6.3	Quartz	14	160	64	1.23
6.3	Iron Oxide	14	25	0	0.938

The scaling procedure employed verifies the initial assumption that the differences in the P_c-S curves in Figure 11 were due to differences in operative contact angle and wettability of the two sands. It is noted that scaling to IFT alone is insufficient to achieve agreement with the quartz pH=6.3 P_c-S curve (figure not shown). It also verifies that the operative contact angles and wettabilities of the pH 6.3 iron oxide and the pH 3.2/3.6 quartz and iron oxide curves were all similar.

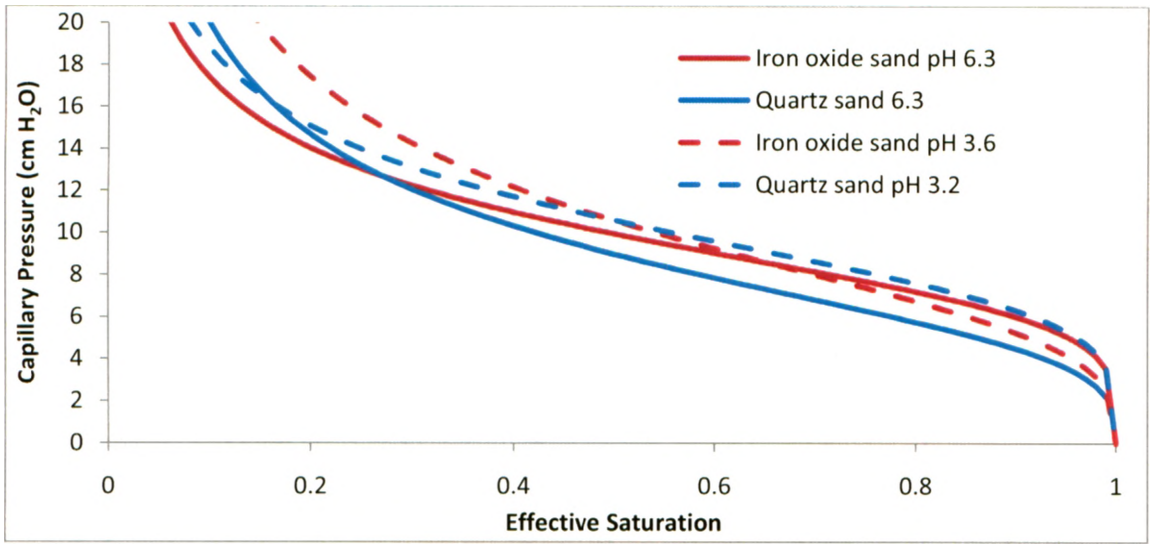

Figure 23: P_c-S relationships scaled to iron oxide pH 6.3 for quartz and iron oxide sands at a pH of 3.2, 3.6 and 6.3 where $[DDA]_T$ =0.0027M.

3.3.3. Flow Cell Experiment

Representative flow cell experimental results for a similar boundary capillary pressure are presented in Figure 14a for pH 3.5 (left) and 14b for pH 6.8 (right). The spatial distribution of PCE occurrence is obtained digitally as described in Section 3.2.6. The figure reveals that PCE was distributed throughout all of the quartz sand at pH 6.8 but was unable to enter the iron oxide-coated sand. This observed difference in DNAPL entry pressures and migration pathways are consistent with the observed differences at both the pore scale (contact angles of 150^{o} and 24^{o} for quartz at iron oxide, respectively) and the P_c-S curves measured at the REV scale. It is calculated that the boundary condition pictured in Figure 14a corresponds to equivalent P_c at the base of the iron oxide of 6.2 cm water. The data from Table 6 (i.e., the pH 6.3 curves from Figure 11) reveals that the predicted effective water saturation at this P_c is greater than 0.9 for iron oxide but approximately 0.35 for quartz.

At pH 3.5, no significant distinction in equilibrium PCE height was observed between the two sand types. This, too, is consistent with the experiments at both of the other scales: at pH 3.5 the two advancing contact angles are very similar (30^{o} and 24^{o} for the iron oxide and quartz, respectively) and the P_c-S curves were also similar.

Figure 14a reveals some noisy data at the edges of the iron oxide lens in the pH 3.5 system. This poor performance of the LTV system in this region in this experiment is attributed to the light transmission properties along a sharp iron oxide/quartz interface. Nevertheless, careful excavation of the sandbox in 1cm increments at the completion of the experiment confirmed that PCE was present inside the entire iron oxide middle lens

as well as the quartz for the pH 3.5 experiment. It also confirmed the validity of the PCE segregation presented in Figure 14b (right) for pH 6.8.

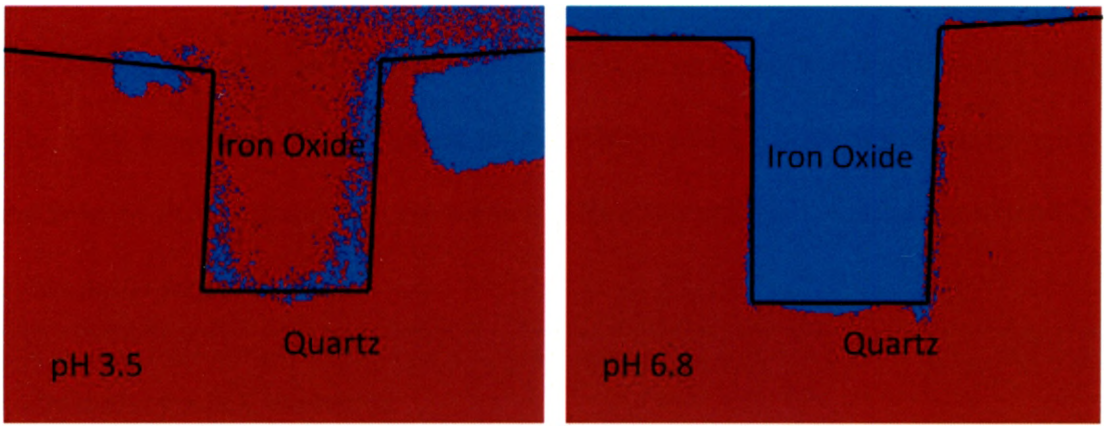

Figure 14: Fluid distributions in flow cell experiments at a) pH 3.5 and b) pH 6.8 and c) a photo of the surface of the flow cell. In figures a and b red represents PCE saturated porous media and blue represents water saturated porous media. P_c at the base of the pH 3.5 sandbox = 9.9 cm H_2O and at the base of the pH 6.8 sandbox = 9.1 cm H_2O.

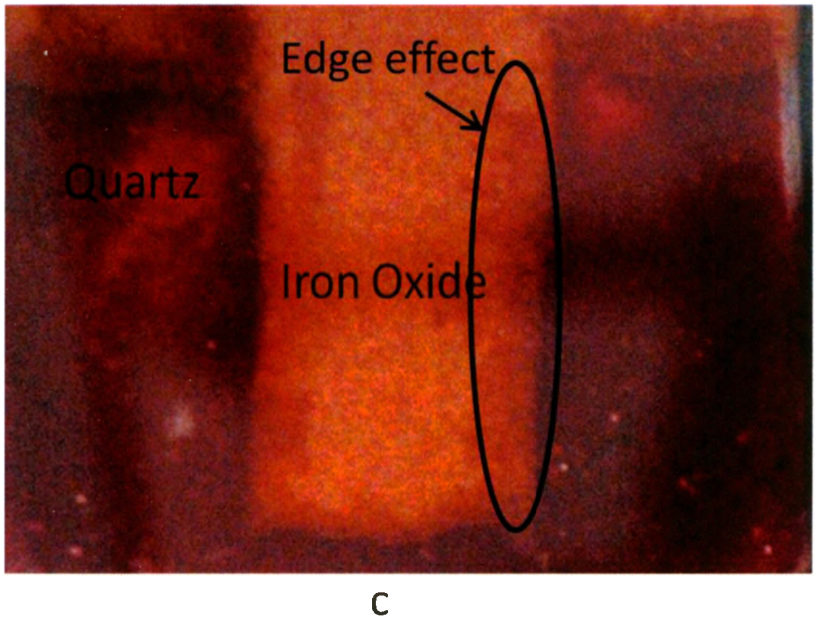

Pictures were also taken without the LTV system to visually confirm the spatial distribution seen in the computer enhanced images. Figure 14c displays a photo taken of the pH 6.8 flow cell at the exact same capillary pressure conditions as 14b. A thin layer of PCE between the flow cell wall and the iron oxide sand can be identified in Figure 14c. The LTV procedure did not detect this thin layer of PCE and excavation revealed that the layer of PCE remained on the surface of the flow cell wall and did not extend in to the iron oxide sand.

3.4.Summary and Conclusion

To the author's knowledge, this study is the first to demonstrate that wettability is sensitive to the minerals present on the soil surface at neutral pH under the scenario of a release of chlorinated solvent comingled with surface active chemicals. It was demonstrated that the organic base would alter the wettability of the quartz surface and not the iron oxide due to differences in surface charge properties.

At the scale of a single drop, an iron oxide surface remained hydrophilic in the pH range $3.5 < pH < 7.5$, whereas quartz, while also hydrophilic at low pH values, exhibited strong NAPL-wetting behavior at near-neutral pH values with DDA. Hysteresis was observed in the contact angle experiments for both quartz and iron oxide surfaces. However at neutral pH the iron oxide surface exhibited larger than expected hysteresis, remaining strongly hydrophilic as the droplet advanced but switching to hydrophobic as the droplet receded. Capillary pressure-saturation experiments with quartz and iron oxide-coated sands revealed that the pore scale wettability similarities at low pH and the wettability differences at near-neutral pH were both reflected in REV-scale constitutive functions.

The influence of these wettability effects on macroscopic DNAPL penetration of porous media were confirmed in flow cell experiments. At pH 6.8, under identical boundary capillary pressures, PCE entered and displaced the majority of water in the quartz sand and was unable to enter the iron oxide-coated sand. This wettability-dependent flow behaviour agreed with predictions from the measured P_c-S curves and illustrated the macroscopic manifestation of the contact angle measurements. In addition the significant hysteresis present on iron oxide surfaces at neutral pH suggest that while water drainage behavior for quartz and iron oxide sands may be different, water imbibition behavior may be similar.

The experiments performed showcase the significant effect that mineral isoelectric points may have on NAPL wettability in the presence of surface active chemicals. While this study focused on examining the differences between quartz and iron oxide surfaces, similar non-uniform behaviour is expected when DDA/NAPL interacts with subsurface minerals exhibiting a variety of isoelectric points and pH varies between those points. Quartz is a very common mineral and the literature has focused on its wettability, however an accurate conceptual model for DNAPL in the subsurface should account for minerals with dissimilar isoelectric points.

Simplifying assumptions were employed in this study such as the use of: uniform, homogeneous soil types free from organic carbon, reagent grade chemicals, a chemically pure aqueous phase, monovalent salts and iron oxide coatings which may be different from iron oxides found in the field. Nevertheless the conclusions made in this study with regards to the role of the solid's isoelectric point in determining DNAPL/surfactant/water

wettability are expected to be applicable to real subsurface systems containing a broad range of minerals. These real systems may include various minerals in a well mixed fractional wetting system or distinct blocks and layers of minerals as seen in the flow cell experiments.

These results have significant implications for DNAPL distribution in the field, especially at sites such as dry cleaning facilities or waste solvent disposal areas where DNAPL/surfactant mixtures are likely to be found. The distribution of minerals, as well as the site's aqueous pH value, may have a significant impact on DNAPL source zone architecture. Commonly occurring minerals that exhibit dissimilar isoelectric points from quartz include iron, aluminum and manganese oxides among others listed in Table 3. Even if a small fraction of soil grains present at a site possess different isoelectric points then the common assumption of homogeneous wetting behavior (either hydrophilic or hydrophobic) should be reconsidered.

3.5. References

Bauters, T. W. J., et al. (2000), Physics of water repellent soils, *Journal of Hydrology.*, *231*, 233-243.

Birak, P. S., and C. T. Miller (2009), Dense non-aqueous phase liquids at former manufactured gas plants: Challenges to modeling and remediation, *Journal of Contaminant Hydrology*, *105*(3-4), 81-98.

Bob, M. M., et al. (2008), A modified light transmission visualization method for DNAPL saturation measurements in 2-D models, *Advances in Water Resources*, *31*(5), 727-742.

Bradford, S. A., et al. (2000), Dissolution of residual tetrachloroethylene in fractional wettability porous media: correlation development and application, *Journal of Contaminant Hydrology*, *45*(1-2), 35-61.

Buckley, J., and Y. Liu (1998), Some mechanisms of crude oil/brine/solid interactions, *Journal of Petroleum Science and Engineering*, *20*(3-4), 191-202.

Buckley, J., and Lord, DL (2003), Wettability and morphology of mica surfaces after exposure to crude oil, *Journal of Petroleum Science and Technology*, *39*(3-4), 261-273.

Cassie, A.B.D. (1948), Permeability to water and water vapour of textiles and other fibrous materials. *Discuss. Faraday Soc.* 3 (11), 239– 243.

Cornell, R. M., Schwetmann, U., (2003), *The iron oxides : structure, properties, reactions, occurrences and uses*, 2 ed., WILEY-VCH Verlag GmbH & Co. KGaA, Weinheim.

Darnault, C. J. G., et al. (1998), Visualization by light transmission of oil and water contents in transient two-phase flow fields, *Journal of Contaminant Hydrology*, *31*(3-4), 337-348.

Demond, A. H., and P. V. Roberts (1991), Effect of interfacial forces on 2-phase capillary pressure saturation relationships, *Water Resources Research*, *27*(3), 423-437.

Demond, A. H., et al. (1994), Effect of cationic surfactants on organic liquid-water capillary pressure-saturation relationships, *Water Resources Research*, *30*(2), 333-342.

Desai, F. N., et al. (1992), The influence of surfactant sorption on capillary pressure-saturation relationships, in *Transport and Remediation of Subsurface Contaminants: Colloidal, Interfacial and Surfactant Phenomena*, edited, pp. 133-148, American Chemical Society, Washington, D.C.

Dou, W., et al. (2008), Characterization of DNAPL from the US DOE Savannah River site, *Journal of Contaminant Hydrology*, *97*(1-2), 75-86.

Dwarakanath, V., et al. (2002), Influence of wettability on the recovery of NAPLs from alluvium, *Environ. Sci. Technol.*, *36*(2), 227-231.

Feldman S.B., C. S., and Lucian W. Zelazny (2008), Soil Mineralogy, in *Encylopedia of Soil Science*, edited by W. Chesworth, pp. 678-685, Springer, Dordrecht.

Gerhard, J. I., and B. H. Kueper (2003), Capillary pressure characteristics necessary for simulating DNAPL infiltration, redistribution, and immobilization in saturated porous media, *Water Resources Research*, *39*(8), 17.

Grant, G. P., et al. (2007), Multidimensional validation of a numerical model for simulating a DNAPL release in heterogeneous porous media, *Journal of Contaminant Hydrology*, *92*(1-2), 109-128.

Harrold, G., et al. (2001), Wettability changes in trichloroethylene-contaminated sandstone, *Environmental Science and Technology*, *35*(7), 1504-1510.

Harrold, G., et al. (2005), The impact of additives found in industrial formulations of TCE on the wettability of sandstone, *Journal of Contaminant Hydrology*, *80*(1-2), 1-17.

Hsu, H.-L., and A. H. Demond (2007), Influence of organic acid and organic base interactions on interfacial properties in NAPL-water systems, *Environmental Science and Technology*, *41*(3), 897-908.

Jackson, R. E., and V. Dwarakanath (1999), Chlorinated degreasing solvents: Physical-chemical properties affecting aquifer contamination and remediation, *Ground Water Monit. Remediat.*, *19*(4), 102-110.

Jeong, S. W., et al. (2002), Effects of pure and dyed PCE on physical and interfacial properties of remedial solutions, *J. Hazard. Mater.*, *95*(1-2), 125-135.

Johnson, P. R., et al. (1996), Colloid transport in geochemically heterogeneous porous media: Modeling and measurements, *Environ. Sci. Technol.*, *30*(11), 3284-3293.

Lord, D., et al. (1997), Influence of organic acid solution chemistry on subsurface transport properties. 2. capillary pressure−saturation, *Environmental Science and Technology*, *31*(7), 2052-2058.

Lord, D.L , et al. (2000), Effects of organic base chemistry on interfacial tension, wettability and capillary pressure in multiphase subsurface waste systems, *Transport in Porous Media*, *38*(1-2), 79-92.

Lord, D. L. (1999), Influence of organic acid and base solution chemistry on interfacial and transport properties of mixed wastes in the subsurface, Ph.D. thesis, 190 pp, University of Michigan, United States -- Michigan.

Lord, D. L., et al. (2005), Comparison of capillary pressure relationships of organic liquid-water systems containing an organic acid or base, *Journal of Contaminant Hydrology*, *77*(3), 195-208.

Martin, A. R., and G. P. Fulton (1958), *Drycleaning Technology and Theory*, Textile Book Publishers, New York.

Mayer, A. S., and S. M. Hassanizadeh (2005), *Soil and Groundwater Contamination: Nonaqueous Phase Liquids*, American Geophysical Union, Washington, D.C.

McNeil, J. D., et al. (2006), Quantitative imaging of contaminant distributions in heterogeneous porous media laboratory experiments, *Journal of Contaminant Hydrology*, *84*(1-2), 36-54.

Mercer, J. W., and R. M. Cohen (1990), A review of immiscible fluids in the subsurface: Properties, models, characterization and remediation, *Journal of Contaminant Hydrology*, *6*(2), 107-163.

Michael Stokes, M. A., Srinivasan Chandrasekar, Ricardo Motta (1996), A Standard Default Color Space for the Internet - sRGB, edited, p. 1, World Wide Web Consortium.

National Research Council (2005), *Contaminants in the Subsurface: Source Zone Assessment and Remediation*, 1 ed., The National Academies Press, Washington D.C.

Niemet, M. R., and J. S. Selker (2001), A new method for quantification of liquid saturation in 2D translucent porous media systems using light transmission, *Advances in Water Resources*, *24*(6), 651-666.

O'Carroll, D. M., et al. (2004), Infiltration of PCE in a system containing spatial wettability variations, *Journal of Contaminant Hydrology*, *73*(1-4), 39-63.

O'Carroll, D. M., et al. (2005a), Prediction of two-phase capillary pressure-saturation relationships in fractional wettability systems, *Journal of Contaminant Hydrology*, *77*(4), 247-270.

O'Carroll, D. M., et al. (2005b), Exploring dynamic effects in capillary pressure in multistep outflow experiments, *Water Resources Research*, *41*(11), 14.

Parks, G. (1965), The isoelectric points of solid oxides, solid hydroxides, and aqueous hydroxo complex systems, *Chemical Reviews*, *65*(2), 177-198.

Powers, S., et al. (1996), Wettability of NAPL-contaminated sands, *Journal of Environmental Engineering*, *122*(10), 889-896.

Powers, S. E., and M. E. Tamblin (1995), Wettability of porous-media after exposure to synthetic gasolines, *Journal of Contaminant Hydrology*, *19*(2), 105-125.

Ryder, J., and A. Demond (2008), Wettability hysteresis and its implications for DNAPL source zone distribution, *Journal of Contaminant Hydrology*, *102*(1-2), 39-48.

Ryer, A. (1998), Light Measurement Handbook, International Light, Newbury, MA.

Shinoda, K. z. (Eds.) (1967), *Solvent properties of surfactant solutions*, Marcel Dekker Inc. , New York.

Singh, U., and G. Uehara (1999), Electrochemistry of the Double Layer: Principles and Applications to Soils, in *Soil Physical Chemistry*, edited, pp. 1-46, CRC Press, Boca Raton.

Sposito, G. (1989), *The Chemistry of Soils*, Oxford University Press, New York.

Tuck, D. M., et al. (2003), Organic dye effects on dense nonaqueous phase liquids (DNAPL) entry pressure in water saturated porous media, *Water Resour. Res.*, *39*(8), 1207

van Genuchten, M. T. (1980), Closed-form equation for predicting the hydraulic conductivity of unsaturated soils, *Soil Science Society of America Journal*, *44*(5), 892-898.

Wang, H. G., et al. (2008), Locally-calibrated light transmission visualization methods to quantify nonaqueous phase liquid mass in porous media, *Journal of Contaminant Hydrology*, *102*(1-2), 29-38.

Zheng, J., and Powers, SE (1999), Organic bases in NAPLs and their impact on wettability, *Journal of Contaminant Hydrology*, *39*(1-2), 161-181.

Zheng, J., et al. (2001), Asphaltenes from Coal Tar and Creosote: Their Role in Reversing the Wettability of Aquifer Systems, *Journal of Colloid and Interface Science*, *244*(2), 365-371.

Chapter 4

Conclusions

4.1.Summary and Conclusion

The work presented in this study demonstrates that the wettability of chlorinated solvent/surface active chemical mixtures is sensitive to the minerals present on the soil surface. The wettability of quartz and iron oxide surfaces was compared using a representative chlorinated solvent/organic base mixture. The surface activity of the organic base used (DDA) has been well documented [*Hsu and Demond*, 2007; *Lord et al.*, 2000; *Lord et al.*, 2005] and its ability to alter the DNAPL/water/soil interfacial properties depends on surface isoelectric properties and speciation. The cationic form of DDA being responsible for most of the wettability alterations seen in literature [*Hsu and Demond*, 2007; *Lord et al.*, 2000; *Lord et al.*, 2005]. Thus it was conjectured that the organic base would alter the wettability of the quartz surface and not the iron oxide in the pH range between their isoelectric points. This would be due to the presence of a negative charge on the quartz surface to which the DDA could sorb and a positive charge on the iron oxide which would not adsorb the cationic DDA.

In the pH range tested (3.2-7.5) the iron oxide surface remained in all the experiments performed while the quartz became strongly NAPL-wetting at neutral pH values. Significant differences were seen in both the PCE advancing contact angles and hysteresis of the contact angle. Quartz exhibited hysteresis throughout the entire pH range while the iron oxide surfaces became hysteretic only at neutral pH values.

Differences measured in the contact angle at neutral pH values translated into differences in the measured P_c-S relationships. At lower pH values where the contact angles were very similar, so were the P_c-S curves. In a small two dimensional flow cell similar results were encountered. At the neutral pH value of 6.8 the PCE migrated up through the NAPL-wetting quartz sand and failed to enter the hydrophilic iron oxide sand whereas at a low pH value of 3.5 the NAPL exhibited no preference for either sand. These results were directly compared to the multi-step outflow experiments and were found to correlate strongly to the measured P_c-S curves.

The isoelectric point of the solid was shown to impact DNAPL wettability in the presence of an organic base. Thus the common assumption that the subsurface is homogeneously wetting has been considered and found inadequate for situations in with DNAPL/surface active chemical mixtures exist and in which various minerals are present with varying isoelectric points.

4.2. Implications

These results have potentially substantial implications for DNAPL distribution in the field. An increasing number of DNAPL waste sites are being identified as containing DNAPL/surfactant mixtures [*Dou et al.*, 2008; *Dwarakanath et al.*, 2002; *Jackson and Dwarakanath*, 1999] and the distribution of minerals may have a substantial impact on DNAPL source zone architecture and remediation efforts. If a wide range of mineral types are present then the common assumption of homogeneous wetting behavior (either hydrophilic or hydrophobic) may be insufficient to accurately assess system behaviours and should be reconsidered

4.3. Recommendations for Further Work

Numerous simplifications and assumptions were employed in this study that may limit the direct applicability of these results to the field. Such simplifications include the use of: uniform, homogeneous soil types free from organic carbon, a relatively simple DNAPL/organic base mixture and iron oxide coatings which may be different from iron oxides found in the field. As such the study discussed here needs to be expanded to better represent both real wastes in the subsurface and real distributions of natural soil minerals. Specific recommendations for future work include:

1) Examining any potential wettability alterations on iron oxide surfaces by organic acids such as octanoic acid. Studies have shown that quartz remains hydrophilic in the presence of organic acids, due to their anionic nature [*Lord et al.*, 1997]. As iron oxide surfaces are positively charged over a greater range of pH values than quartz, the possibility exists for organic acids to render iron oxide NAPL-wetting while quartz remains strongly hydrophilic.
2) Further studying the effect of mineral heterogeneity on the wettability of real complex waste NAPLs by examining both water drainage and imbition behaviours with mixtures of different soil minerals

4.4. References

Dou, W., et al. (2008), Characterization of DNAPL from the US DOE Savannah River Site, *Journal of Contaminant Hydrology*, *97*(1-2), 75-86.

Dwarakanath, V., et al. (2002), Influence of wettability on the recovery of NAPLs from alluvium, *Environ. Sci. Technol.*, *36*(2), 227-231.

Hsu, H.-L., and A. H. Demond (2007), Influence of organic acid and organic base interactions on interfacial properties in NAPL-water systems, *Environmental Science and Technology*, *41*(3), 897-908.

Jackson, R. E., and V. Dwarakanath (1999), Chlorinated degreasing solvents: Physical-chemical properties affecting aquifer contamination and remediation, *Ground Water Monit. Remediat.*, *19*(4), 102-110.

Lord, D., et al. (1997), Influence of organic acid solution chemistry on subsurface transport properties. 2. capillary pressure−saturation, *Environmental Science and Technology*, *31*(7), 2052-2058.

Lord, D.L , et al. (2000), Effects of organic base chemistry on interfacial tension, wettability and capillary pressure in multiphase subsurface waste systems, *Transport in Porous Media*, *38*(1-2), 79-92.

Lord, D. L., et al. (2005), Comparison of capillary pressure relationships of organic liquid-water systems containing an organic acid or base, *Journal of Contaminant Hydrology*, *77*(3), 195-208.

Appendices

Appendix A

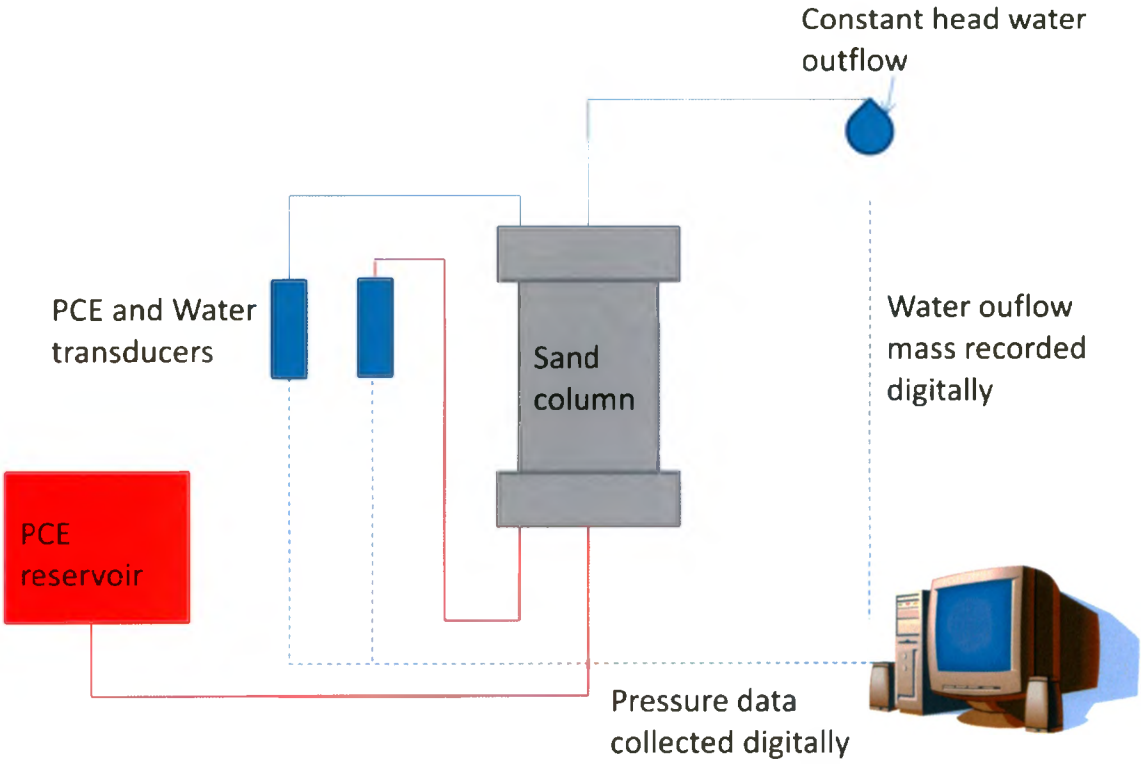

Figure A.1: Diagram of the multi-step outflow apparatus used for measuring primary drainage Pc-S relationships

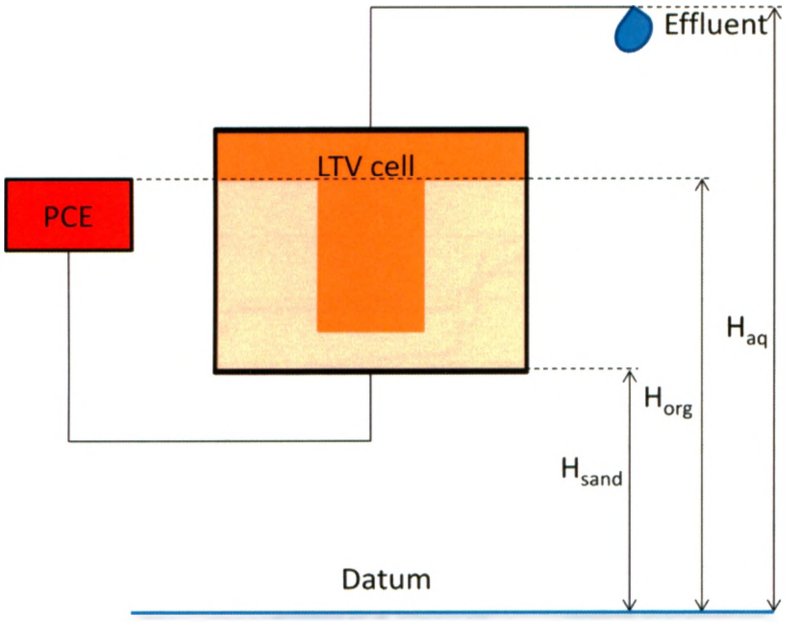

Figure A.2: Setup used for the flow cell experiments

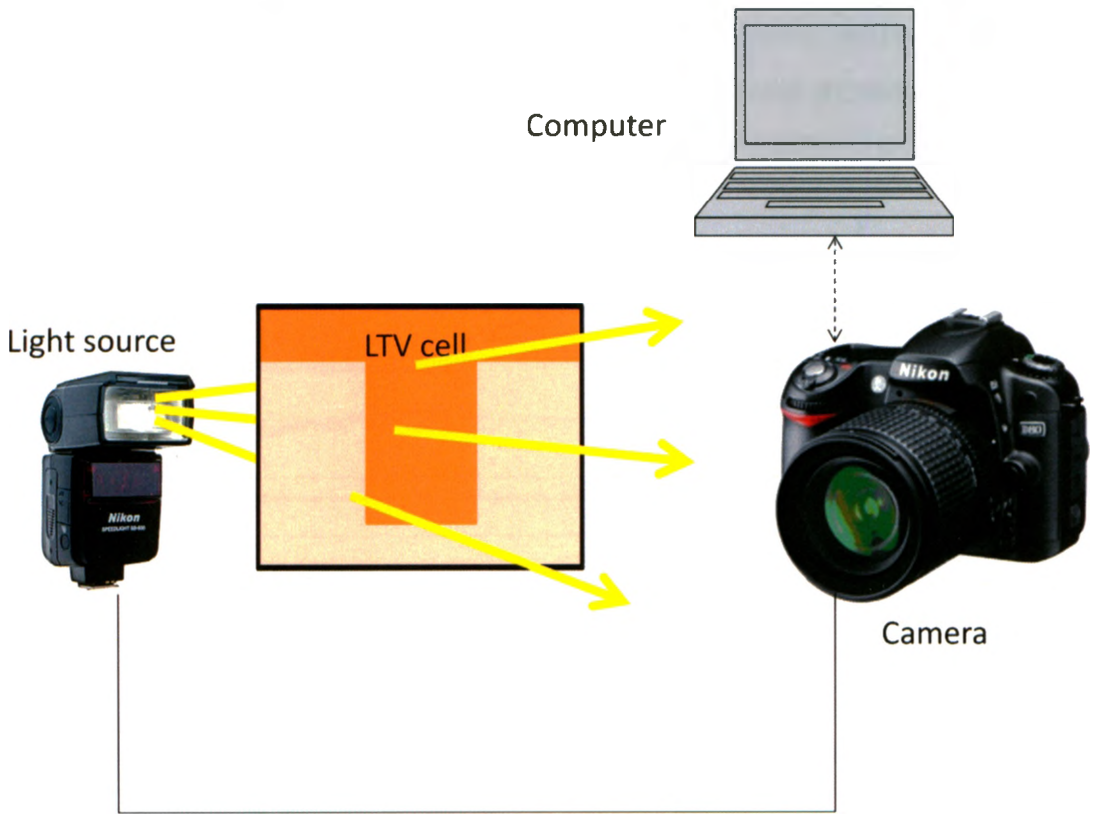

Figure 3: Light transmission visualization setup for the flow cell experiments

Appendix B

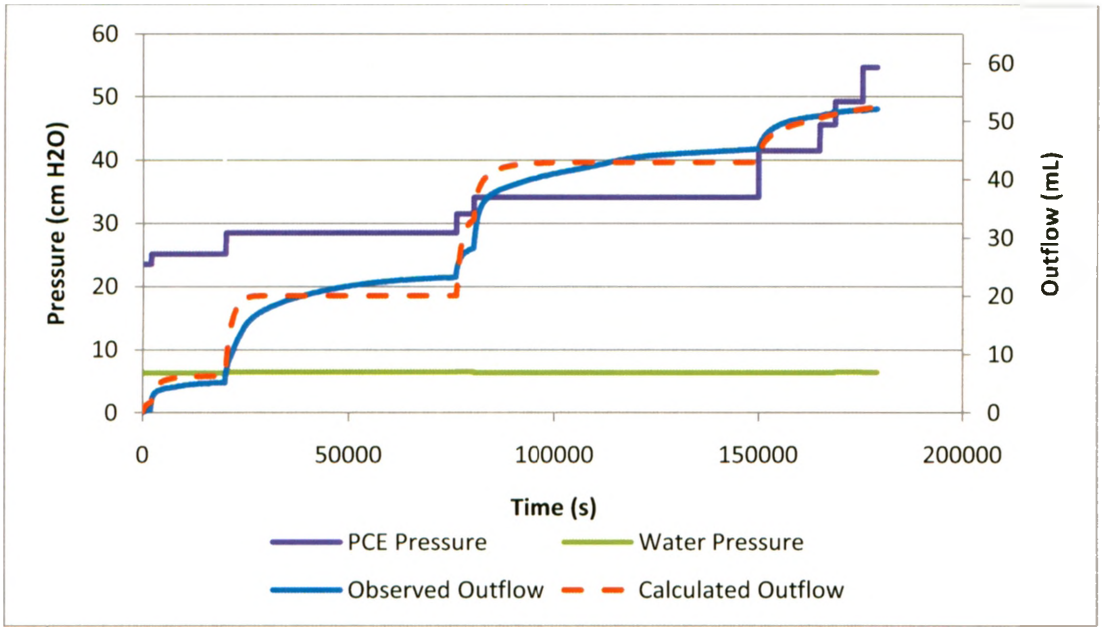

Figure B.1: Comparison of observed and fit cumulative water outflow for the iron oxide pH 6.3 MSO. PCE and water boundary pressures are also presented.

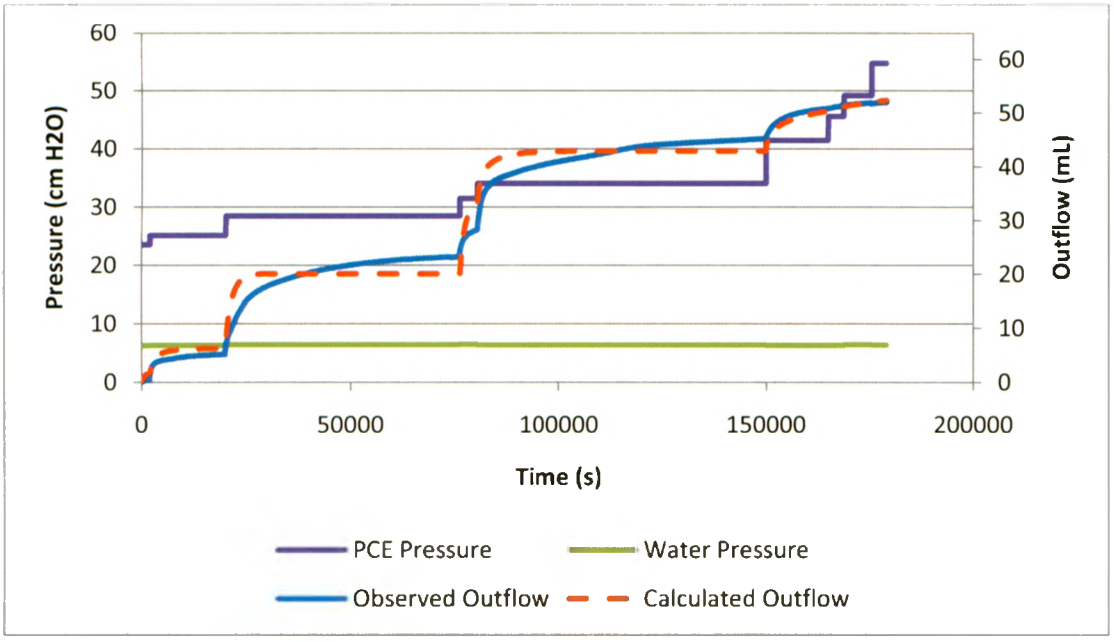

Figure B.4: Comparison of observed and fit cumulative water outflow for the quartz pH 6.3 MSO. PCE and water boundary pressures are also presented.

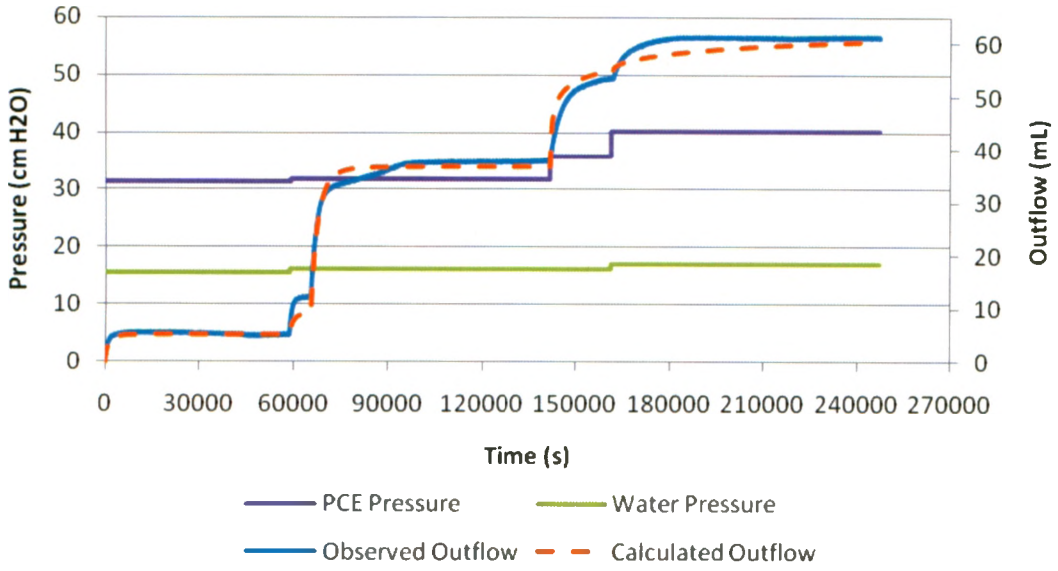

Figure B.5: Comparison of observed and fit cumulative water outflow for the quartz pH 3.2 MSO. PCE and water boundary pressures are also presented.

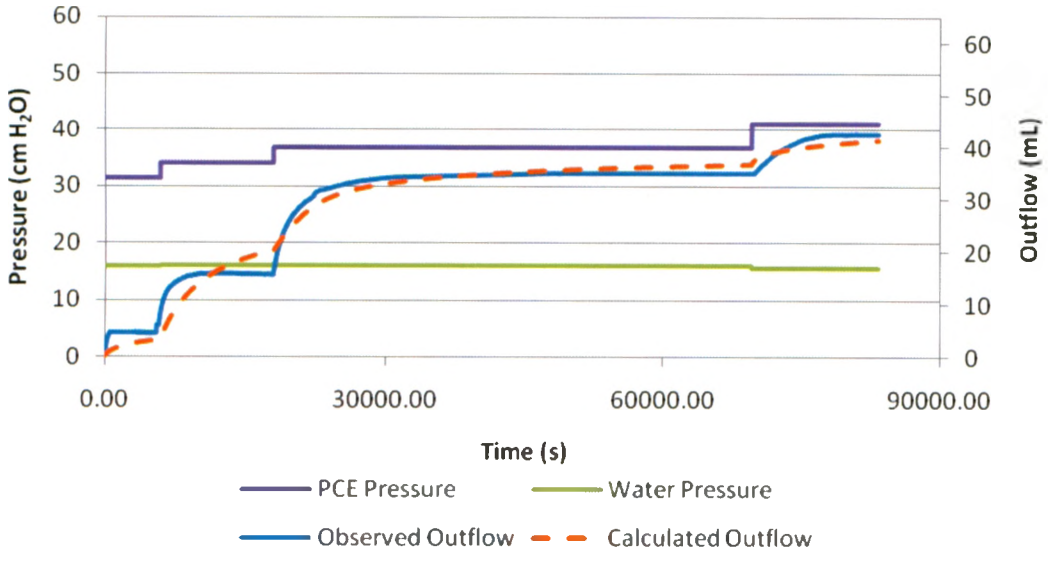

Figure B.6: Comparison of observed and fit cumulative water outflow for the iron oxide pH 3.6 MSO. PCE and water boundary pressures are also presented.

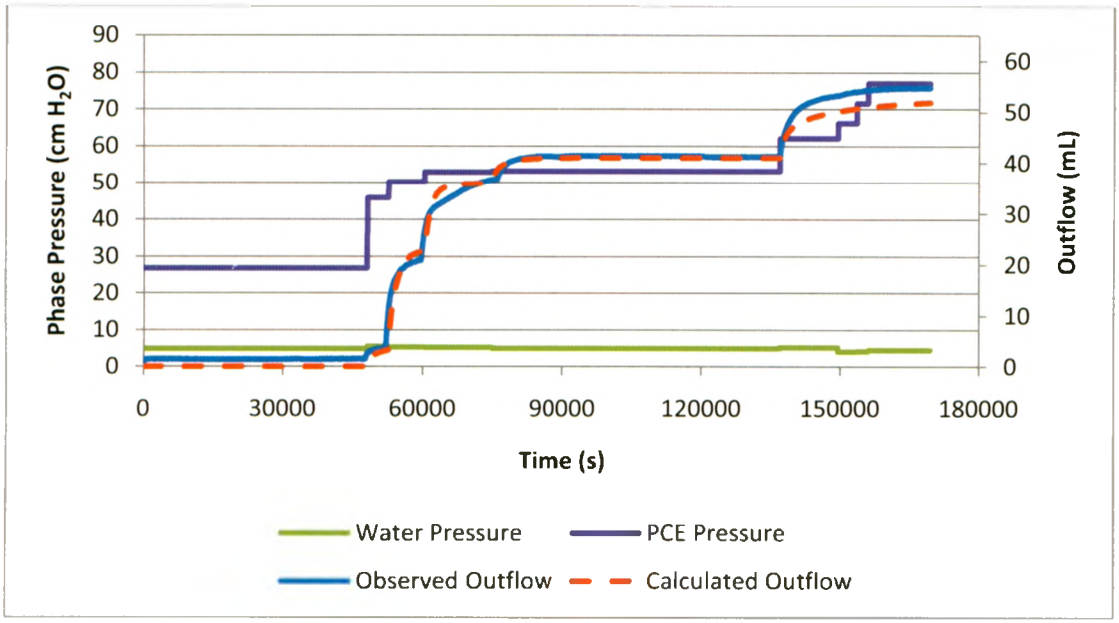

Figure B.5: Comparison of observed and fit cumulative water outflow for the pure PCE/Water/Quartz MSO. PCE and water boundary pressures are also presented.

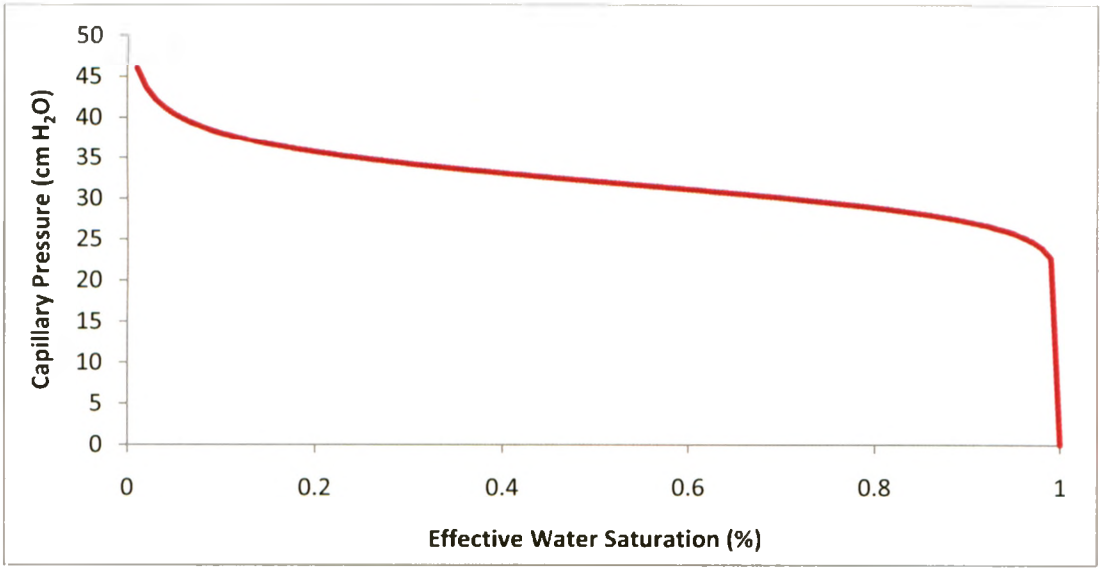

Figure B.6: Estimated Pc-S relationship for pure PCE/water on F70 quartz sand.